Please cite this article as: Li, S, Liu, R, Gao, Z. and Yang, L (2021) Integrated train dwell time regulation and train speed profile generation for automatic train operations on high-density metro lines: A distributed optimal control method. Transportation Research Part B. 148, 82-105. https://doi.org/10.1016/j.trb.2021.04.009

Integrated train dwell time regulation and train speed profile generation for automatic train operations on high-density metro lines: A distributed optimal control method

Shukai Li[a], Ronghui Liu[b], Ziyou Gao[a], Lixing Yang[a]

[a]*State Key Laboratory of Rail Traffic Control and Safety, Beijing Jiaotong University, Beijing, 100044, China*
[b]*Institute for Transport Studies, University of Leeds, Leeds LS2 9JT, U.K.*

Abstract

The wide-spread application of automatic train operation (ATO) system on metro lines allows short service headways, high-density operations and high operation efficiency. This paper addresses real-time train control for ATO when faced with disturbances or disruptions in its operations. More specifically, the paper focuses on the design of integrated train dwell time regulation and speed profile generation in real-time and in response to dynamic changes in the operation environment. A nonlinear optimal control model is formulated in a rolling horizon scheme that incorporates three key operating elements: train timetable, passenger load and train speed profile. The objective is to simultaneously improve headway regularity and reduce the total energy consumptions. To satisfy the real-time control requirement for ATO system, a decomposition method based on the alternating direction method of multipliers (ADMM) is designed to divide the original optimization problem into many sub-problems, one for each train, which can then be computed in a distributed manner. Moreover, to address the non-convexity issue, a relax-round-polish process is developed to deal with the formulated nonlinear optimal control problem with convex objective over non-convex constraints in order to find the approximate solutions quickly for the embedded applications. The combined result is an ADMM-based heuristic algorithm. The effectiveness of the proposed model and solution algorithm is demonstrated using real-world data from the Changping Line of Beijing Metro. The results show that the proposed distributed and embedded optimization algorithm is able to significantly enhance the robustness and reliability of real-time train control in automated high-density metro lines.

Keywords: Metro lines, Train regulation, Speed profile generation, Alternating direction method of multipliers, Nonlinear optimal control

1. Introduction

Urban rail-based metro system has been hailed as an effective solution to relieve the traffic congestion pressure in a metropolis due to its capacity, reliability, and energy-consumption efficiency. Increasing urbanization leads to a massive increase in passenger demand for urban metro system. This trend is particularly acute in metropolises such as Beijing, Tokyo, and New York. On the supply side, the daily operations of many automated high-density metro transport systems are subject to frequent disturbances or disruptions,

*Corresponding author.
Email address: R.Liu@its.leeds.ac.uk (Ronghui Liu)

Please cite this article as: Li, S, Liu, R, Gao, Z. and Yang, L (2021) Integrated train dwell time regulation and train speed profile generation for automatic train operations on high-density metro lines: A distributed optimal control method. Transportation Research Part B. 148, 82-105. https://doi.org/10.1016/j.trb.2021.04.009

ranging from complex signalling problems to relatively simple door-operating problems, all of which contribute to the significant degradation of the system's level of service. In a high traffic density metro system, the delay of a train at one station leads to increased passenger accumulation and train dwell time in the downstream station, which in turn adds to further delay to the train. To assist in improving the operational efficiency and service reliability, automatic train operation (ATO) system has been applied in many of these high-frequency and high-density metro lines to help monitor and control the operation of all the trains in the system (Xun et al., 2019; Yin et al., 2020). An integral part of ATO is a robust timetable including train running time between stations and dwell time at stations that balances the passenger demand and train service supply, and a desired train running speed profile on line segment that drives the train safely and efficiently to the timetabled time. The speed profile can be optimized to minimize the energy consumption, giving the trains traction and braking power, the conditions on the track such as track geometry and speed limits, and on the train load (Ye and Liu, 2016, 2017).

In practice, the timetable (mainly the station dwell times) and train running speed profiles are adjusted constantly in real-time to respond to changes in passenger demand and/or other disturbances in the system (Wu et al., 2016, 2019; Li et al., 2019). There is a need to coordinate the real-time dwell time change and speed profile regeneration to balance the tradeoff between the operation efficiency and energy consumption. This paper is to investigate this interrelated control problem of train dwell time regulation and speed profile generation. In addition, the real-time nature of the control problem requires computationally efficient solutions. The distributed control methods that divide a large control problem into a set of smaller control problems to be calculated through multiple processors, have been successfully applied in many fields to meet the real-time performance requirement. To support the automatic train operation system, this paper is to design an efficient distributed optimal control framework for real-time, integrated train dwell time regulation and speed profile generation, with the aim to simultaneously improve the operation efficiency and reduce the energy consumption on automated high-density metro lines.

1.1. Literature review

Unpredictable incidents occur frequently on metro lines. When that happens, the planned train schedule can no longer meet the original optimized objectives and a train reschedule process is required to mitigate the disruption caused by the incident to the system. During the last few years, a great amount of literature is devoted to the development of effective methods for train rescheduling problems of metro system (Caimi et al., 2007; Mannino and Mascis, 2009; Corman et al., 2012; Kecman et al., 2013; Cacchiani et al., 2014; Kang et al., 2015; Corman and Meng, 2018).

Specifically, for ATO systems, automatic train regulation (ATR) has been developed as a key function of modern urban metro signaling system for effectively recovering train delays. ATR works by dynamically regulating the dwell time and running time of trains to reduce the redundant slack time and meanwhile improve the capacity utilization. In recent years, a number of efficient ATR methods have been developed for the operations of metro lines. For example, Van Breusegem et al. (1991) developed a state-space modeling framework and adopted a linear quadratic programming method to design the train regulation strategy that stabilizes the metro system with respect to uncertain disturbances. To improve the quality of passenger service, Chang and Thia (1996) investigated an online train timetable rescheduling method for urban rapid rail transit after a sudden passenger load disturbance. Goodman and Murata (2001) adopted a traditional optimization method to adjust the metro line system with the aim of improving the passenger service level. By considering the non-linear characteristics of passenger demand, Lin and Sheu (2011) applied a heuristic

Please cite this article as: Li, S, Liu, R, Gao, Z. and Yang, L (2021) Integrated train dwell time regulation and train speed profile generation for automatic train operations on high-density metro lines: A distributed optimal control method. Transportation Research Part B. 148, 82-105. https://doi.org/10.1016/j.trb.2021.04.009

dynamic program algorithm to solve the train regulation problem that reduces the total train delay of metro lines. Applying a discrete Markovian process to describe the stochastic passenger flow, Li et al. (2016b) proposed a robust control model to design a robust optimal train running time and dwell time regulation strategy that tracks the nominal train timetable under disturbances. Taking energy consumptions into consideration, Sheu and Lin (2012) designed a dual heuristic programming-based train regulation method to achieve both a better schedule/headway adherence and a higher energy efficiency.

Separately, to meet the real-time control requirement and to incorporate the updated system information, the model-based predictive control (MPC) methods have been adopted to solve the train regulation problems. Fernandez et al. (2006) proposed a predictive optimization model for the metro train dwell time and running time adjustment problem, in which the regulation strategy was calculated over a given predictive time horizon in a rolling optimization manner. Li et al. (2016a) adopted a MPC to design robust train optimal regulation in a looped metro line with uncertainties in passenger arrival flow. They show that the method guaranteed not only the robust stability of the metro line, but also the minimization of a given system control performance. Moaveni and Najafi (2018) introduced a discrete event nonlinear train dynamic model for a looped metro and employed a robust model predictive controller with operational constraints for the automatic train regulation problem. For the goal of simultaneously improving the operational efficiency and the energy consumption efficiency, a real-time efficient MPC algorithm was proposed to generate the optimal train regulation strategy after disturbance in Zhang et al. (2019). By using a fuzzy passenger arrival rate to address the uncertainties for the passenger demand, Wang et al. (2019) developed a fuzzy predictive controller to track the nominal train scheduling and reduce delays. Li et al. (2018) applied a distributed MPC combined with a dual decomposition method for the ATR problem considering the transfer passenger flow in complex metro networks. The method can effectively divide the previous network optimal control problem into a set of small metro line optimal control sub-problems to improve the computation efficiency.

Most existing literature on ATR tends to focus on adjusting the timetable to reduce the total train delays. However, for a complete automatic operation for the trains, one needs to consider not only the train timetable decision at a macroscopic level, but also train speed profile generation at a microscopic level. Recently, a few literatures have investigated the integration of train scheduling and train speed profile with the aim to improve operation efficiency while reducing train energy consumption. To optimize both train schedule and train speed profile, Li and Lo (2014) proposed an energy-efficient operation model of metro lines that improves the braking regenerative energy utilization and reduces the train tractive consumption under constraints of the train schedule. By considering the regenerative energy consumption, Su et al. (2015) developed a joint train motion control model to calculate the train departure time and the optimal running profile that utilizes regenerative energy to reduce the line's overall energy consumption. Yin et al. (2017) employed a time-space network representation to formulate the train scheduling and control problem that reduces the passenger waiting time and minimizes the energy consumption under dynamic passenger demands. For real-life practical applications, ATR control methods need to be able to respond in real-time to updated information. So far, very little literature can be found to deal with the integration of the train rescheduling and speed profile generation in real time. In this paper, an effort has been made to develop efficient control strategy for the integrated ATR and speed profile generation. Moreover, we consider ATR for multiple trains and develop a distributed optimization algorithm to deal with complex constraints inherent in such problems. To achieve the goal of reducing the computation complexity and to design on-line solutions that take into account real-time updated information, we develop a distributed MPC method by splitting the coupled optimal control problem into a set of small-scale optimal control sub-problems, where

Please cite this article as: Li, S, Liu, R, Gao, Z. and Yang, L (2021) Integrated train dwell time regulation and train speed profile generation for automatic train operations on high-density metro lines: A distributed optimal control method. Transportation Research Part B. 148, 82-105. https://doi.org/10.1016/j.trb.2021.04.009

each subsystem only needs to solve a low-dimensional optimization problem for its control action (Boyd et al., 2011; Vasirani and Ossowski, 2011; Timotheou et al., 2015; Yao et al., 2019). We present the design of this completely distributed optimal control method for the dynamic train regulation and speed profile generation of metro system, in such a way as to realize an efficient and fast computational performance.

1.2. Proposed approach and contributions

Whilst there have been many works on the study of train regulation methods and integration of train scheduling and speed control methods for metro lines, to the best of our knowledge, very few have addressed the integrated problem of train regulation and speed profiles generation for real-time operations and with multiple trains in a metro system. Ye and Liu (2016) incorporated a train timetable adjustment function into an energy-efficient train control algorithm, for an off-line optimization on an isolated single train. While ATO in the modern metro system has the capability to monitor and control the operations of trains in real time, designing and operating multiple trains' dwell time and speed profile generation in real-time is challenging, not only because of the complex coupled relationship among the timetable, passenger load and the speed profile, but also the computational efficiency required for its real-time implementation. This study takes on the challenges and develops a distributed and embedded optimal control method for the integrated train dwell time regulation and speed profile generation for automated train operations on high-density metro lines. The specific contributions of this paper are presented as follows.

(1) Compared to the existing ATR problem which adjusts only the train timetable, our proposed integrated train dwell time regulation and speed profile generation for real-time application is a step-change towards system-wide safe and efficient operations of automated metro systems. The designed real-time control strategy can be directly implemented to the existing ATO system to enable it to better respond to the frequent disturbances in the real-life operation of metro lines, and improve headway regularity and reduce total energy consumptions.

(2) Compared to the existing centralized optimization method (Li and Lo, 2014; Su et al., 2015), in this study, we realize an embedded application of dynamic train regulation and speed profile generation in a completely distributed optimal control framework, which allows fast computation and facilitates its real-time application. The distributed control framework is based on an improved alternating direction method of multipliers (ADMM) with a relax-round-polish process to find approximate solutions to the problem quickly. The original optimization problem is decomposed into many sub-problems, one for each train. The sub-problems can then be computed in a distributed manner fast and effectively. The inherent modularity of the distributed computation mechanism allows for easy expansion of the control system, and it has a greater tolerance to train failures and higher robustness than centralized optimization method.

The main features of our paper, as compared to existing literature, are summarized in Table 1. By comparison, this paper considers the integrated train regulation and speed profile generation problem, which provides a more general and practical framework for train control problems than those consider simply train regulation problems (Van Breusegem et al., 1991; Fernandez et al., 2006; Lin and Sheu, 2010; Sheu and Lin, 2012). Based on an alternating direction multipliers based decomposition method, a completely distributed optimal control framework is designed in this paper, which achieves a faster and more flexible computational performance than the traditional centralized optimization method (Li and Lo, 2014; Su et al., 2015; Yin et al., 2017), and which makes our proposed control method more practical for real-time ATO applications.

The rest of this paper is organized as follows. In Section 2, the integration problem for the train dwell regulation and speed profile generation is presented. In Section 3, the distributed and embedded optimal

Please cite this article as: Li, S, Liu, R, Gao, Z. and Yang, L (2021) Integrated train dwell time regulation and train speed profile generation for automatic train operations on high-density metro lines: A distributed optimal control method. Transportation Research Part B. 148, 82-105. https://doi.org/10.1016/j.trb.2021.04.009

Table 1: Comparison to key existing literature.

Characteristics	Problem	Objective	Passenger flow	methodology	Solution way
Van Breusegem et al. (1991)	Train regulation	Operation efficiency	Constant	State feedback control	Centralized
Fernandez et al. (2006)	Train regulation	Operation efficiency	Constant	Model predictive control	Centralized
Lin and Sheu (2010)	Train regulation	Operation efficiency	Constant	Heuristic dynamic programming	Centralized
Sheu and Lin (2012)	Train regulation	Operation efficiency and energy consumption	Constant	Dual heuristic programming	Centralized
Li and Lo (2014)	Train scheduling and speed control	Operation efficiency and energy consumption	Constant	Genetic algorithms	Centralized
Su et al. (2015)	Train scheduling and speed control	Waiting time and energy consumption	Constant	Bisection method	Centralized
Yin et al. (2017)	Train scheduling and speed control	Operation efficiency and energy consumption	Variable	Mixed-integer linear programming	Centralized
This paper	Train regulation and speed profile generation	Headway regularity and energy consumption	Variable	Alternating direction method of multipliers based decomposition	Distributed

control solution approach is designed. In Section 4, numerical examples are provided to demonstrate the effectiveness of the proposed methods. We conclude this paper in Section 5.

2. Train dwell regulation and speed profile generation problem

We consider a classical configuration of a two-track line with two terminus stations (one track in each direction) on an automated high-density metro transport system as shown in Figure 1. During the operation, a train arrives at a station to service the alighting and boarding passengers. When completing this service at the station, the train needs to determine the speed profile and the departure time to the next station. This decision process is usually required to complete within 3 seconds in practical applications. When making the decision, three key elements need to be considered, which include the current train timetable, passenger load and train speed profile for all trains in the whole metro line system. There are complex interplays among these three key elements. The train dwell time is dependent on the number of boarding and alighting passengers, while the headway between trains influences the number of passengers waiting to board. The passenger load on the train affects train's energy consumption, which in turn will affect the speed profile generation that determines the train running time. This study incorporates the complex and coupled relationships among these three key elements in the design of train dwell time regulation and speed profile generation and for their real-time applications. In this section, we first present models of passenger dynamic, train dynamic and train speed curves, and then formulate the optimal control model for the integrated problem of train headway regulation and speed profile generation.

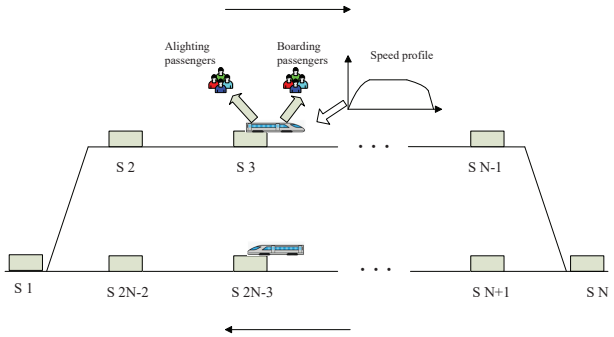

Figure 1. An illustration of metro line structure.

Please cite this article as: Li, S, Liu, R, Gao, Z. and Yang, L (2021) Integrated train dwell time regulation and train speed profile generation for automatic train operations on high-density metro lines: A distributed optimal control method. Transportation Research Part B. 148, 82-105. https://doi.org/10.1016/j.trb.2021.04.009

To facilitate the analysis of this study, we introduce the following assumptions.

First, we assume that for the considered metro operation system, trains follow each other based on a given sequence while train crossing and overtaking are prohibited. This is a reasonable assumption for the majority of metro lines where train crossing and overtaking are not facilitated. In addition, the stop-skipping operation is not considered in the proposed model.

Second, train dwell time is approximated as a linear function with the number of actual passengers boarding and alighting. In metro lines, dwell time is the major cause of vehicle pairing, similar to bus bunching effect (Fonzone et al., 2015; Schmöcker et al., 2016). From an empirical study, Eberlein et al. (2001) found a linear relationship between the dwell time and the number of passengers boarding and alighting.

Third, over the study time period (e.g. between $07:00-10:00$), the passenger arrival rates vary with stations and with time. During each decision time period (typically 3-5min), however, an average fixed passenger arrival rate is assumed. The passenger alighting at any station is modelled as a portion of passengers on the train approaching that station. Thus, the passenger arrival rates and alighting fractions will fluctuate over time and vary from station to station.

Fourth, for each inter-station, the set of speed profiles are assumed to be pre-given and we need to choose one from the speed profile set. In the actual ATO system, a set of the speed profiles are saved in the system in advance for each inter-station based on the operation condition. When the train departs from a station, one of the speed profiles would be chosen from the speed curves set according to the train operation feedback information. If one train is delayed, it can choose a speed profile with a shorter running time so as to reduce such a delay. Another consideration in choosing a particular speed profile is energy consumption since different speed profiles will generate different amounts of energy consumption.

The indices and parameters used throughout this paper are listed in Table 2.

2.1. Modelling passenger dynamics

In an automated high-density metro line, when a train arrives at the station, it opens the doors and services the boarding and alighting passengers. When finishing this service, it closes the doors and departs from the station. To describe this service process clearly, we first construct the passenger flow dynamics model. We use the passenger load on each train, denoted by L_j^i, as the state variable of passenger dynamics. The dynamic equation for the changing of passenger load (on-board) from one station to the next station can be presented as follows.

$$L_j^i = L_{j-1}^i + b_j^i - a_j^i, \tag{1}$$

where b_j^i is the number of boarding passengers for train i at station j and a_j^i is the corresponding number of alighting passengers, $i = 1, 2, \ldots,\ i \in \mathrm{M}$, where M is the set of trains on the line, and $j = 1, 2, \ldots,\ N$, where N is the number of stations on the line. Similar to (Wu et al., 2017), a_j^i is assumed to be proportional to the number of passenger on board, and is given as $a_j^i = c_j^i L_{j-1}^i$. The alighting fraction c_j^i can be estimated or predicted by the real-time automatic fare collection (AFC) system data.

Table 2: Indices and parameters used in the paper.

Please cite this article as: Li, S, Liu, R, Gao, Z. and Yang, L (2021) Integrated train dwell time regulation and train speed profile generation for automatic train operations on high-density metro lines: A distributed optimal control method. Transportation Research Part B. 148, 82-105. https://doi.org/10.1016/j.trb.2021.04.009

$i = 1, 2, \ldots,\ i \in \mathrm{M}$:	Indices of all the operating trains;
$j = 1, 2, \ldots, N$:	Indices of the stations;
N_i:	The set of neighboring trains of train i;
α, β:	The coefficients in the objective;
System Parameters	
H:	The scheduled headway;
λ_j^i:	Passenger arrival rate at station j for train i;
c_j^i:	Passenger alighting fractions at station j for train i;
$l_{\max}$:	Maximum capacity for each train;
$W_{\max}$:	Maximum capacity at the platform;
ρ:	Alighting/boarding time per passenger;
m_{1i}:	Mass of train i without passengers;
m_{2i}:	Average masse per passenger;
$g_{j,k}^i$:	The running time to the speed profile k for train i between stations j and $j+1$;
$e_{j,k}^i$:	The energy consumption per mass unit to the speed profile k for train i between stations j and $j+1$;
$H_{\min}$:	Minimum allowable safety headway;
$\bar{u}_s$:	Maximum allowable train dwell time regulation;
tr_j^i:	Transfer passenger number at transfer station j for train i;
State Variables	
D_j^i:	Departure time of train i from station j;
L_j^i:	Passenger load of train i departing from station j.;
W_j^i:	Number of passengers left behind at station j when train i departs from station j.;
a_j^i:	Boarding passengers for train i when arriving at station j;
b_j^i:	Alighting passengers for train i when arriving at station j;
r_j^i:	Running time of train i between stations j and $j+1$;
s_j^i:	Dwell time of train i at station j;
$w_{r_j}^i$:	The disturbance to the running time of train i between stations j and $j+1$;
$w_{s_j}^i$:	The disturbance to the dwell time of train i at stations j;
Decision Variables	
$u_{s_j}^i$:	Dwell time adjustment for train i between stations j and $j+1$;
$u_{r_j}^i$:	Control variable to running time of train i between stations j and $j+1$;
$y_{j,k}^i$:	0-1 binary variable, if the k-th speed curve for train i between stations j and $j+1$ is chosen, $y_{j,k}^i = 1$; otherwise, $y_{j,k}^i = 0$;
$x_{j,k}^i$:	The extra auxiliary real variable that equals to $L_j^i y_{j,k}^i$;
p_j^i:	The extra auxiliary real variable in linearized process of the nonlinear term $\min(\cdot)$;
δ_j^i:	The extra auxiliary binary variable in linearized process of the nonlinear term $\min(\cdot)$.

During peak hours, it is common that some passengers would fail to board on the first arrival train and have to wait for the next train due to the capacity limitation of the trains. We introduce a state variable, denoted by W_j^i, to represent the number of passengers left behind at station j when train i departures from station j. The dynamic evolution equation for the number of passengers left behind at the station is

Please cite this article as: Li, S, Liu, R, Gao, Z. and Yang, L (2021) Integrated train dwell time regulation and train speed profile generation for automatic train operations on high-density metro lines: A distributed optimal control method. Transportation Research Part B. 148, 82-105. https://doi.org/10.1016/j.trb.2021.04.009

formulated as follows.

$$W_j^i = W_j^{i-1} + \lambda_j^i(D_j^i - D_j^{i-1}) + tr_j^i - b_j^i, \tag{2}$$

where D_j^i is the departure time of train i from station j. λ_j^i is the passenger arrival rate at station j, which can be estimated by the real-time AFC data. The term $\lambda_j^i(D_j^i - D_j^{i-1})$ denotes the accumulated number of passenger arrivals during the interval between two departures. tr_j^i is the number of transfer passengers from other lines when station j is a transfer station, which is an external parameter and is given in advance according to the real-time monitor system.

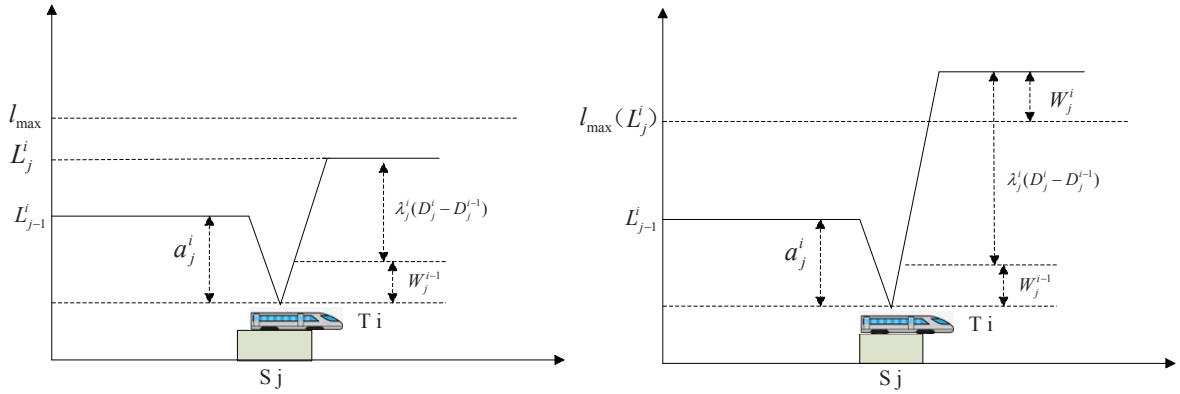

Figure 2. A diagrammatic illustration of the dynamic changes in passenger flow, where (a) is the case with spare capacity on the train and (b) is the case with a full load on the train.

Along with the state variable W_j^i for the number of passengers left behind at the station, the number of boarding passengers b_j^i is formulated as

$$\begin{aligned} b_j^i &= \min(W_j^{i-1} + \lambda_j^i(D_j^i - D_j^{i-1}) + tr_j^i, l_{\max} - (L_{j-1}^i - a_j^i)) \\ &= \min(W_j^{i-1} + \lambda_j^i(D_j^i - D_j^{i-1}) + tr_j^i, l_{\max} - (L_{j-1}^i - c_j^i L_{j-1}^i)), \end{aligned} \tag{3}$$

where $l_{\max}$ denotes the maximum train capacity. The term $W_j^{i-1} + \lambda_j^i(D_j^i - D_j^{i-1}) + tr_j^i$ represents the total waiting passenger number when train i arrives at station j, while the term $l_{\max} - (L_{j-1}^i - a_j^i)$ represents the surplus capacity of train i when arriving at station j. The number of boarding passengers is the smaller one between the waiting passenger number and the surplus capacity on the train. If the surplus capacity is larger than the waiting passenger number, the arrival train will service all the waiting passengers, otherwise, there will be passengers left behind at the station. This dynamic changes in passenger flows is illustrated in Figure 2, where Figure 2(a) is the case that the surplus capacity on the train is more than the waiting passenger number, while Figure 2(b) is the case that the surplus capacity is smaller than the waiting passenger number.

By combining equations (1)-(3), the passenger flow dynamics of on-board and waiting at the platform can be formulated as follows.

$$\begin{aligned} L_j^i &= L_{j-1}^i + \min(\tilde{W}_j^{i-1}, \tilde{L}_{j-1}^i) - c_j^i L_{j-1}^i, \\ W_j^i &= W_j^{i-1} + \lambda_j^i(D_j^i - D_j^{i-1}) + tr_j^i - \min(\tilde{W}_j^{i-1}, \tilde{L}_{j-1}^i), \end{aligned} \tag{4}$$

Please cite this article as: Li, S, Liu, R, Gao, Z. and Yang, L (2021) Integrated train dwell time regulation and train speed profile generation for automatic train operations on high-density metro lines: A distributed optimal control method. Transportation Research Part B. 148, 82-105. https://doi.org/10.1016/j.trb.2021.04.009

where $\tilde{W}_j^{i-1} = W_j^{i-1} + \lambda_j^i(D_j^i - D_j^{i-1}) + tr_j^i$ and $\tilde{L}_{j-1}^i = l_{\max} - (L_{j-1}^i - c_j^i L_{j-1}^i)$.

The above formulation authentically captures the dynamic interactions between the waiting passengers on the platform and the train load. It shows explicitly that the passenger load is affected by the train timetable $D_j^i - D_j^{i-1}$, revealing the coupled relationship between passenger load and train timetable. If the train's capacity is available, it will take all waiting passengers. Passengers can board a train to its maximum capacity, while those who failed-to-board will be added to the waiting passengers for the next train.

2.2. Modelling train dynamics

In an automatic train operation system, the state variables representing train operation include train departure time, train dwell time, and train speed profile. Trains' departure time and dwell time are typically used to measure the operation efficiency, while the train running speed is linked to the energy consumption. With real-time feedback information of train departure time and passenger flow from stations, the function of ATO is to determine the train speed profile to, and train dwell time at, the next station. The ultimate objective is to achieve both high operation efficiency and energy efficiency. We choose the train departure time D_j^i for train i from station j as the state variable for the train dynamic. Specifically, for the high-frequency metro system, train dwell time depends on the passenger flow, and train running time is related to the speed profile generation. At first, the evolution model of train dynamic is formulated as follows

$$D_j^i = D_{j-1}^i + r_{j-1}^i + s_j^i, \tag{5}$$

where r_{j-1}^i is the running time between station $j-1$ and j for train i, and s_j^i is the dwell time of train i at station j.

Train running time between stations is dependent on the speed profile and can be affected by inevitable disturbances, such as signal failure. Based on this, train running time r_{j-1}^i is formulated as

$$r_{j-1}^i = {u_r}_{j-1}^i + {w_r}_{j-1}^i, \tag{6}$$

where ${u_r}_{j-1}^i$ is the control variable that is directly related to the speed profile generation. Different values of ${u_r}_{j-1}^i$ represent different speed profiles for train i during the inter-station, which needs to be determined. Variable ${w_r}_{j-1}^i$ is introduced to represent the delay to the running time caused by disturbances.

In the metro line system, dwell time variability is the main cause for the vehicle pairing effect. It is strongly affected by the number of passengers boarding and alighting, more so than on mainline railways where small variations in station dwell time can be relatively easily absorbed by the long journey times between stations. We consider busy metro lines where alighting precedes boarding, the dwell time s_j^i is then, affected by the combined number of alighting and boarding passengers and is modelled as

$$\begin{aligned} s_j^i &= \rho(b_j^i + a_j^i) + {u_s}_j^i + {w_s}_j^i \\ &= \rho(\min(\tilde{W}_j^{i-1}, \tilde{L}_{j-1}^i) + c_j^i L_{j-1}^i) + {u_s}_j^i + {w_s}_j^i, \end{aligned} \tag{7}$$

where ρ is the average alighting/boarding time per passenger, ${w_s}_j^i$ denotes delay to the dwell time caused by the passenger variants or disturbance, and ${u_s}_j^i$ is the dwell time regulation that needs to be determined. The train dwell time formulation of (7) takes explicit account of train capacity when determining the number of passengers who can actually board, leading to a more realistic representation of the effect of alighting/boarding passenger flow to the dwell time.

Please cite this article as: Li, S, Liu, R, Gao, Z. and Yang, L (2021) Integrated train dwell time regulation and train speed profile generation for automatic train operations on high-density metro lines: A distributed optimal control method. Transportation Research Part B. 148, 82-105. https://doi.org/10.1016/j.trb.2021.04.009

By combining (5)-(7), the train dynamic is formulated as

$$D_j^i = D_{j-1}^i + \rho(\min(\tilde{W}_j^{i-1}, \tilde{L}_{j-1}^i) + c_j^i L_{j-1}^i) + {u_s}_j^i + {u_r}_{j-1}^i + \bar{w}_j^i, \tag{8}$$

where $\bar{w}_j^i = {w_r}_{j-1}^i + {w_s}_j^i$. This formulation characterizes the dynamic coupling relationship between the passenger evolution dynamics and the train motion dynamics and describes the instability in actual metro line system operations due to the accumulation of passenger flows: if one train is delayed, the accumulated passenger flow can further extend the delay propagation to other trains behind.

2.3. The speed profile generation with energy saving

With disturbances to the operation of trains, the train's speed profile during the inter-station running will also need to be re-generated automatically and in real-time. Normally, in the practical automatic train control systems, several different speed profiles are stored that correspond to different running times. These are pre-calculated optimal train speed profiles with the objective of minimizing energy consumption using an off-line optimization. The operational decision, in practice, is to determine the most appropriate speed profile according to the real-time operation information. For example, if the train is delayed at the station, it would choose a speed profile with a shorter running time to the next station, but with a higher energy consumption. There is a practical need to realize a tradeoff between the operational efficiency and energy efficiency when determining the speed profile.

A speed profile can be divided into four intervals: traction, cruising, coasting and braking intervals. Given different inter-station running times, different speed profiles that minimize energy consumption can be generated, as shown in shown as Figure 3. In this study, we consider that there are m pre-calculated speed profiles for each inter-station segment, which correspond to m running times. The decision is to determine the speed profile from the given set with different train energy consumption and running time.

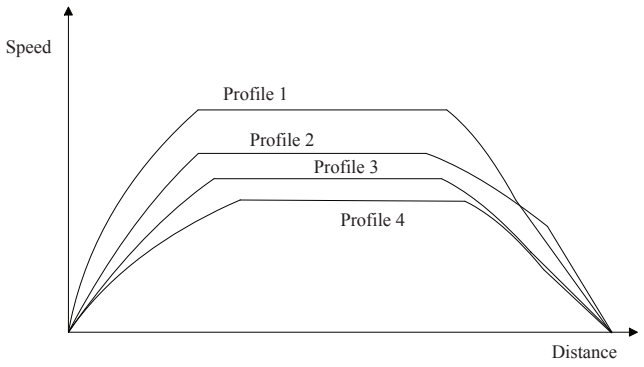

Figure 3. An illustration of a set of pre-given speed profiles for an inter-station running.

To accurately describe the relationship among the speed profile, train running time and train energy consumption, we introduce a binary variable $y_{j,k}^i$ to represent whether the speed profile k is chosen for train i between station j and $j+1$ or not. If the k-th speed profile is chosen, $y_{j,k}^i = 1$, otherwise, $y_{j,k}^i = 0$. Since there is only one speed profile can be chosen for train j between station j and $j+1$, we have the following constraint

$$\sum_{k=1}^{m} y_{j,k}^i = 1, \quad i \in M,\ j = 1, 2 \ldots, N. \tag{9}$$

Please cite this article as: Li, S, Liu, R, Gao, Z. and Yang, L (2021) Integrated train dwell time regulation and train speed profile generation for automatic train operations on high-density metro lines: A distributed optimal control method. Transportation Research Part B. 148, 82-105. https://doi.org/10.1016/j.trb.2021.04.009

By considering that each speed profile corresponds to one running time control variable, it is convenient to convert the running time control variable ${u_r}_j^i$ into the selection of the train speed profiles. Based on this, there are m running time control decisions corresponding to different speed profiles. We denote $g_{j,k}^i$ to represent the running time corresponding to the speed profile k. The control variable for running time ${u_r}_j^i$ can be converted into the following form

$$ {u_r}_j^i = \sum_{k=1}^{m} y_{j,k}^i g_{j,k}^i, \quad \sum_{k=1}^{m} y_{j,k}^i = 1, \tag{10} $$

where $g_{j,k}^i$ is a pre-given constant.

For each given speed profile, the total energy consumption will change with train load, the latter varies with the passenger load on the train. Taking into account of train's traction and resistance force, the energy consumption for the train during the inter-station can be calculated by the following equation.

$$ E = \int_0^T rc(t)v(t)\mathrm{d}t = m\int_0^T (a(t) + f(t))v(t)\mathrm{d}t \tag{11} $$

where m is the train mass, $rc(t)$ and $v(t)$ are traction force and speed of the train at time t, while $a(t)$ and $f(t)$ are acceleration and resistance, respectively. Equation (11) shows that, for a given inter-station speed profile, the energy consumption is proportional to the mass of the train. As the train load varies from inter-station to inter-station, we adopt a notation of energy consumption per mass unit for each given speed profile. Then, under the control variable ${u_r}_j^i$, the energy consumption per mass unit for train i between station j and $j+1$ is obtained as

$$ E_j^i = \sum_{k=1}^{m} y_{j,k}^i e_{j,k}^i, \quad \sum_{k=1}^{m} y_{j,k}^i = 1, \tag{12} $$

where $e_{j,k}^i$ is a given constant, which represents the energy consumption per mass unit for each speed profile k. Compared to the traditional nonlinear function for the calculation of the energy consumption, the model provides a simple linear form with a binary variable, which can be easily implemented in the actual real-time train control.

In this study, we explicitly consider the time variant of passenger load L_j^i. Thus the mass of train changes in different inter-stations due to the variable passenger load. The corresponding energy consumption for each train is formulated as follows.

$$ \hat{E}_j^i = (m_{1i} + m_{2i}L_j^i)\sum_{k=1}^{m} y_{j,k}^i e_{j,k}^i = m_{1i}\sum_{k=1}^{m} y_{j,k}^i e_{j,k}^i + m_{2i}L_j^i\sum_{k=1}^{m} y_{j,k}^i e_{j,k}^i, \quad \sum_{k=1}^{m} y_{j,k}^i = 1, \tag{13} $$

where m_{1i} is the mass of train i without passengers and m_{2i} is average mass per passenger. The above train energy consumption model combines the passenger load state and the speed profile variable, which lead to a nonlinear form that needs to be linearized in the following section.

2.4. The real-time optimal control model

To satisfy the real-time requirement of ATO control for train dwell time regulation and speed profile generation, we present an optimal control model in a rolling horizon, discrete-event framework. Since the optimization decision on speed profiles and train dwell time adjustment to the stations downstream is made when a train is ready to depart from a station, we adopt a discrete-event scheme to determine the choice of each decision interval, i.e., each decision interval should cover at least one departure event for each train.

Please cite this article as: Li, S, Liu, R, Gao, Z. and Yang, L (2021) Integrated train dwell time regulation and train speed profile generation for automatic train operations on high-density metro lines: A distributed optimal control method. Transportation Research Part B. 148, 82-105. https://doi.org/10.1016/j.trb.2021.04.009

2.4.1. Rolling horizon scheme

To address the metro ATR problem, our proposed rolling horizon scheme contains two time intervals: an optimization decision interval and a rolling prediction horizon. At each optimization decision interval (decision interval) with the available information of train departure time, passenger load and left passenger at station, an optimal control input is calculated over a pre-specified rolling prediction horizon to minimize a system objective. The decision interval is shorter than the prediction horizon. The computed result within the decision interval is chosen to apply, and at the next optimization interval step, this prediction optimization process is repeated based on the receding horizon (moving horizon) scheme. Specifically, for the operation of high-density metro lines, each decision interval should cover at least one departure event for each train. We can often choose an adequate decision interval (larger than the scheduled headway) to cover at least one departure event for each train. With this interval, the prediction horizon is chosen to cover more departure events for each train to ensure the reliability of the solution. At each decision interval, an optimal control problem is formulated for all the departure events occurring during the prediction horizon, where only the computed result within the decision interval is applied, i.e., one time decision for each train including one speed profile and dwell time adjustment is made. The diagram of the rolling horizon scheme for the real-time metro train control problem is illustrated in Figure 4.

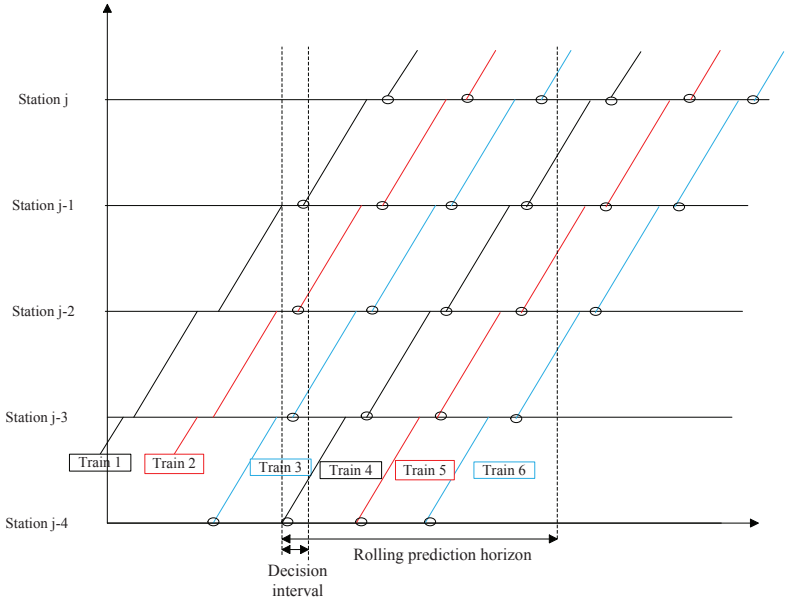

Figure 4. The illustration of the rolling horizon scheme.

Similar to an event-trigger control scheme, when the departure event for a train occurs, a decision stage and optimization interval are triggered and an optimal control problem is formulated and solved to determine the train dwell time adjustment and to generate the train speed profile. At each decision interval h, the set for all the operating trains is $\{i|i \in \mathrm{M}\}$, the set for the available information of train departure time, passenger load and left passenger at station is $\{L_j^i, W_j^i, D_j^i|(L_j^i, W_j^i, D_j^i) \in A_h\}$. Over the prediction horizon, the set for the state and control variables is $\{L_j^i, W_j^i, D_j^i, y_{j,k}^i, u_{sj}^i|(L_j^i, W_j^i, D_j^i, y_{j,k}^i, u_{sj}^i) \in V_h\}$, the set of corresponding stations that each train i departures is denoted as $N_{i,h}$. In such a rolling horizon method, the impact of forecast errors can be limited and corrected by future, updated information at the next decision

Please cite this article as: Li, S, Liu, R, Gao, Z. and Yang, L (2021) Integrated train dwell time regulation and train speed profile generation for automatic train operations on high-density metro lines: A distributed optimal control method. Transportation Research Part B. 148, 82-105. https://doi.org/10.1016/j.trb.2021.04.009

interval.

2.4.2. Objective

While most of the mainline railways operate according to a nominal (timetabled) schedule, it is more important to ensure headway regularity between successive trains for automated high-density metro lines. In light of frequent and uniform metro-type railways services, it is reasonable to assume that passengers are not especially conscious of the timetable. Instead, the passengers are more concerned with the waiting time, and it is known that passengers value their waiting time significantly more than the on-board running time (Goodman and Murata, 2001; Hollander and Liu, 2008). Train headway regularity control is to minimize the deviations of the time intervals between successive trains, and reduce the average waiting time for the passengers (Fernandez et al., 2006; Mannino and Mascis, 2009). Thus, headway regularity has been one of the train regulation objectives for high-density metro lines. Energy efficiency is another important concern for the metro operation, and we take energy saving as another objective. In Beijing Metro, the energy consumption due to train traction force accounts for 50% of all electricity consumption. The overall objective of this study is to improve headway regularity and reduce train traction energy consumption. Based on this, at each decision interval h, the objective over the rolling horizon is formulated as

$$\text{Min} \sum_{i\in M} \sum_{(i,j)|j\in N_{i,h}} \left\{ \alpha(D_j^i - D_j^{i-1} - H)^2 + \beta(m_{1i} + m_{2i}L_j^i) \sum_{k=1}^{m} y_{j,k}^i e_{j,k}^i \right\}. \tag{14}$$

In the above objective, the first term is referred to the headway regularity, which is also related to passenger waiting time, where H is the scheduled headway. The second term is the energy consumption, which is affected by the passenger load and train running time. The objectives of these two terms can be inconsistent. For example, the improvement of headway regularity by reducing running time will increase the energy consumption. The coefficients α, β are employed in (14) to allow trade-offs between operational efficiency (e.g., headway regularity) and costs (energy consumption), to be analyzed and used according to practical objectives.

2.4.3. Constraints

Combining the models of passenger and train dynamics, and speed profile selection as described in Sections 2.1-2.3, the state constraints of train dynamics can be presented as

$$D_j^i = D_{j-1}^i + \rho(\min(\tilde{W}_j^{i-1}, \tilde{L}_{j-1}^i) + c_j^i L_{j-1}^i) + \sum_{k=1}^{m} y_{j-1,k}^i g_{j-1,k}^i + u_{s}{}_j^i + \bar{w}_j^i. \tag{15}$$

The state constraints for the dynamic changes in passenger load number and failed-to-board passenger number can be presented as

$$\begin{aligned} L_j^i &= L_{j-1}^i + \min(\tilde{W}_j^{i-1}, \tilde{L}_{j-1}^i) - c_j^i L_{j-1}^i, \\ W_j^i &= W_j^{i-1} + \lambda_j^i (D_j^i - D_j^{i-1}) + tr_j^i - \min(\tilde{W}_j^{i-1}, \tilde{L}_{j-1}^i). \end{aligned} \tag{16}$$

To ensure the safe operation of metro lines, we need to consider the following minimum headway safety constraint

$$D_j^i - D_j^{i-1} \geq H_{\min}, \tag{17}$$

where $H_{\min}$ is the minimum allowable safety headway.

Please cite this article as: Li, S, Liu, R, Gao, Z. and Yang, L (2021) Integrated train dwell time regulation and train speed profile generation for automatic train operations on high-density metro lines: A distributed optimal control method. Transportation Research Part B. 148, 82-105. https://doi.org/10.1016/j.trb.2021.04.009

To represent the platform capacity, we introduce a maximum capacity constraint of the platform for the number of failed-to-board passengers as follows.

$$W_j^i \leq W_{\max}, \tag{18}$$

where $W_{\max}$ is the maximum capacity at the platform.

For dwell time regulation, we consider the following constraint.

$$0 \leq u_{sj}^{\ i} \leq \bar{u}_s, \tag{19}$$

where $\bar{u}_s$ is the maximum allowable train dwell time regulation.

Finally, for the speed profile generation, one and only one speed profile can be selected for each inter-station train run.

$$y_{j,k}^i = \{0,1\},\ \sum_{k=1}^{m} y_{j,k}^i = 1. \tag{20}$$

2.4.4. The optimal control model

Under objective (14) and constraints (15)-(20), at each decision interval h, recalling the expression of $\tilde{W}_j^{i-1}$ and $\tilde{L}_{j-1}^i$ in equation (4), we can formulate the optimal control model for the integrated train dwell time regulation and speed profile generation problem as follows.

$$\text{Min} \sum_{i\in M} \sum_{(i,j)|j\in N_{i,h}} \left\{ \alpha(D_j^i - D_j^{i-1} - H)^2 + \beta(m_{1i} + m_{2i}L_j^i) \sum_{k=1}^{m} y_{j,k}^i e_{j,k}^i \right\} \tag{21}$$

$$\begin{aligned}\text{s.t. } D_j^i = {} & D_{j-1}^i + \rho(\min(W_j^{i-1} + \lambda_j^i(D_j^i - D_j^{i-1}) + tr_j^i, l_{\max} - (L_{j-1}^i - c_j^i L_{j-1}^i)) + c_j^i L_{j-1}^i) \\ & + \sum_{k=1}^{m} y_{j-1,k}^i g_{j-1,k}^i + u_{sj}^{\ i} + \bar{w}_j^i,\end{aligned} \tag{22}$$

$$L_j^i = L_{j-1}^i + \min(W_j^{i-1} + \lambda_j^i(D_j^i - D_j^{i-1}) + tr_j^i, l_{\max} - (L_{j-1}^i - c_j^i L_{j-1}^i)) - c_j^i L_{j-1}^i, \tag{23}$$

$$\begin{aligned}W_j^i = {} & W_j^{i-1} + \lambda_j^i(D_j^i - D_j^{i-1}) + tr_j^i - \min(W_j^{i-1} + \lambda_j^i(D_j^i - D_j^{i-1}) + tr_j^i, \\ & l_{\max} - (L_{j-1}^i - c_j^i L_{j-1}^i)),\end{aligned} \tag{24}$$

$$D_j^i - D_j^{i-1} \geq H_{\min}, \tag{25}$$

$$W_j^i \leq W_{\max}, \tag{26}$$

$$y_{j,k}^i = \{0,1\}, \tag{27}$$

$$\sum_{k=1}^{m} y_{j,k}^i = 1, \tag{28}$$

$$0 \leq u_{sj}^{\ i} \leq \bar{u}_s. \tag{29}$$

The above formulated optimal control problem at each decision interval h is in fact a nonlinear mixed integer optimization problem. The nonlinear terms $L_j^i y_{j,k}^i$ existing in the objective and $\min(W_j^{i-1} + \lambda_j^i(D_j^i - D_j^{i-1}) + tr_j^i, l_{\max} - (L_{j-1}^i - c_j^i L_{j-1}^i))$ in the constraint can be further linearized by introducing new extra variables according to the linearized process proposed by (Bemporad and Morari, 1999). The following propositions will present the linearized process for the above nonlinear terms.

Please cite this article as: Li, S, Liu, R, Gao, Z. and Yang, L (2021) Integrated train dwell time regulation and train speed profile generation for automatic train operations on high-density metro lines: A distributed optimal control method. Transportation Research Part B. 148, 82-105. https://doi.org/10.1016/j.trb.2021.04.009

Proposition 2.1. *By introducing an auxiliary real variable* $x^i_{j,k} = L^i_j y^i_{j,k}$ *and defining* $l_{\min} = \min(L^i_j)$*, the nonlinear term* $L^i_j y^i_{j,k}$ *is equivalent to following linear inequality.*

$$\begin{aligned} x^i_{j,k} &\le l_{\max} y^i_{j,k}, \\ x^i_{j,k} &\ge l_{\min} y^i_{j,k}, \\ x^i_{j,k} &\le L^i_j - l_{\min}(1 - y^i_{j,k}), \\ x^i_{j,k} &\ge L^i_j - l_{\max}(1 - y^i_{j,k}). \end{aligned} \tag{30}$$

Proposition 2.2. *Let* $f_{\min} = -W_{\max}$ *and* $f_{\max} = l_{\max}$*. By introducing an auxiliary real variable* p^i_j *and a auxiliary binary variable* δ^i_j*, the nonlinear term* $\min(W^{i-1}_j + \lambda^i_j(D^i_j - D^{i-1}_j) + tr^i_j, l_{\max} - (L^i_{j-1} - c^i_j L^i_{j-1}))$ *is equivalent to the linear term* $W^{i-1}_j + \lambda^i_j(D^i_j - D^{i-1}_j) + tr^i_j + p^i_j$ *with the following linear constraints.*

$$\begin{aligned} l_{\max} - (L^i_{j-1} - c^i_j L^i_{j-1}) - W^{i-1}_j - \lambda^i_j(D^i_j - D^{i-1}_j) - tr^i_j &\le f_{\max}(1 - \delta^i_j), \\ l_{\max} - (L^i_{j-1} - c^i_j L^i_{j-1}) - W^{i-1}_j - \lambda^i_j(D^i_j - D^{i-1}_j) - tr^i_j &\ge \varepsilon + (f_{\min} - \varepsilon)\delta^i_j, \\ p^i_j &\le f_{\max}\delta^i_j, \\ p^i_j &\ge f_{\min}\delta^i_j, \\ l_{\max} - (L^i_{j-1} - c^i_j L^i_{j-1}) - W^{i-1}_j - \lambda^i_j(D^i_j - D^{i-1}_j) - tr^i_j - f_{\min}(1 - \delta^i_j) &\ge p^i_j, \\ l_{\max} - (L^i_{j-1} - c^i_j L^i_{j-1}) - W^{i-1}_j - \lambda^i_j(D^i_j - D^{i-1}_j) - tr^i_j - f_{\max}(1 - \delta^i_j) &\le p^i_j. \end{aligned} \tag{31}$$

where ε *is a given small positive scalar.*

With the linearized results in Proposition 2.1 and 2.2, the nonlinear optimal control (21) can be further equivalently converted into a linear quadratic mixed integer programming problem as follows.

$$\text{Min} \sum_{i \in M} \sum_{(i,j)|j \in N_{i,h}} \left\{ \alpha(D^i_j - D^{i-1}_j - H)^2 + \beta(m_{1i} \sum_{k=1}^{m} y^i_{j,k} e^i_{j,k} + m_{2i} \sum_{k=1}^{m} x^i_{j,k} e^i_{j,k}) \right\} \tag{32}$$

$$\text{s.t. } D^i_j = D^i_{j-1} + \rho(W^{i-1}_j + \lambda^i_j(D^i_j - D^{i-1}_j) + tr^i_j + p^i_j + c^i_j L^i_{j-1}) + \sum_{k=1}^{m} y^i_{j-1,k} g^i_{j-1,k} + {u_s}^i_j + \bar{w}^i_j, \tag{33}$$

$$L^i_j = L^i_{j-1} + W^{i-1}_j + \lambda^i_j(D^i_j - D^{i-1}_j) + tr^i_j + p^i_j - c^i_j L^i_{j-1}, \tag{34}$$

$$W^i_j = W^{i-1}_j + \lambda^i_j(D^i_j - D^{i-1}_j) + tr^i_j - (W^{i-1}_j + \lambda^i_j(D^i_j - D^{i-1}_j) + p^i_j), \tag{35}$$

$$\delta^i_j = \{0, 1\}, \tag{36}$$

$$(25) - (29), (30) - (31). \tag{37}$$

Usually, a centralized optimization method is designed to solve the above optimization problem (32). For large metro system size and long prediction time horizon, the computation burden for the above optimization becomes insurmountable, making it practically un-deployable. In practical real-time operations, the embedded optimal control problem needs to be solved within a few seconds while a train is waiting to depart from a station. In addition, the centralized optimization for all the trains during the predictive horizon can also be confined by the communication constraints. For centralized optimization, the whole optimal control design problem has to be made again when a new subsystem is added. For these reasons, it is desirable to design a distributed structure to solve the above optimization problem. The distributed structure requires, both defining fewer and smaller optimal control problems and ensuring the modularity of the solution structure. To meet these requirements, by treating each train as one sub-system, we propose

Please cite this article as: Li, S, Liu, R, Gao, Z. and Yang, L (2021) Integrated train dwell time regulation and train speed profile generation for automatic train operations on high-density metro lines: A distributed optimal control method. Transportation Research Part B. 148, 82-105. https://doi.org/10.1016/j.trb.2021.04.009

a distributed and embedded optimal control algorithm using an alternating direction method of multipliers based decomposition, where each subsystem is updated only from information communicated with its neighbors.

3. The distributed optimal control solution approach

In this section, we present the distributed and embedded optimal control solution approach for the dynamic train regulation and speed profile generation problem. To meet the real-time performance of ATO system, an alternating direction method of multipliers (ADMM) based decomposition is designed to decompose the previous optimal control problem into many subproblems of each train, so that the whole problem can be computed in a distributed manner. ADMM is an augmented Lagrangian method that guarantees convergence with a very mild assumption, which can also realize an improved convergence speed. Moreover, to address the nonconvexity issue and enhance the algorithm performance, an efficient heuristic based on the relax-round-polish process method is developed to cope with the formulated nonlinear optimal control problem with convex objective over non-convex constraints to find approximate solutions quickly for the embedded applications.

3.1. Model decomposition in a distributed manner

Under the ADMM framework, to complete the model decomposition in a distributed manner, we will first reduce the coupling variables into so-called consistency constraints form, and then design the dualization and decomposition process, which are shown in detail below.

3.1.1. Consistency constraints form

For the optimization problem (32), there are coupling constraints (25), (33)-(35) on the departure time variable D_j^i and the left passengers variable W_j^i. To deal with these in a distributed manner, we reduce the coupling variables into consistency constraints by introducing local copies of the variables for each subsystem. The above motion of multiple trains can be regarded as a network with M agents. The agents communicate information with each other based on a fixed graph $G = (V, E)$. The vertex set $E \in V \times V$ represents pairs of agents that are allowed to communicate. The agents i and j are neighbors if $(i, j) \in E$. The set of neighbors of agent i is denoted by $N_i = \{j : (i, j) \in E\}$. In particular, for the above optimization problem (32), each train needs the information of its ahead train. So the set of neighboring trains of each train i is $N_i = i - 1$.

Specifically, we define a new departure time variable $\bar{D}_j^i$ for each train i that includes a copy of its own state D_j^i and also a copy of its neighbors state D_j^{i-1}, i.e., $\bar{D}_j^i = [D_j^i, D_j^{i-1}]$. Similarly, we define a new variable for state $\bar{W}_j^i$ for each train i that includes a copy of its own state W_j^i and also a copy of its neighbors state W_j^{i-1}, i.e., $\bar{W}_j^i = [W_j^i, W_j^{i-1}]$. For example, for train 3, the new variables are $\bar{D}_j^3 = [D_j^3, D_j^2]$ and $\bar{W}_j^3 = [W_j^3, W_j^2]$.

By introducing a new global variable z and letting $\bar{D}^i = \{\bar{D}_j^i |\ j \in N_{i,h}\}$, $L^i = \{L_j^i | j \in N_{i,h}\}$, $\bar{W}^i = \{\bar{W}_j^i | j \in N_{i,h}\}$, $x_k^i = \{x_{j,k}^i | j \in N_{i,h}\}$, $u_s^i = \{u_{sj}^i | j \in N_{i,h}\}$, $y_k^i = \{y_{j,k}^i | j \in N_{i,h}\}$ and $\delta^i = \{\delta_j^i |\ j \in N_{i,h}\}$, the optimization problem (32) can be converted to the following consistency constraints form.

$$\min\ J = \sum_{i \in M} f_i(\bar{D}^i, L^i, \bar{W}^i, x_k^i, p^i, u_s^i, y_k^i, \delta^i) \tag{38}$$

$$\text{s.t. } (\bar{D}^i, L^i, \bar{W}^i, x_k^i, p^i, u_s^i, y_k^i, \delta^i) \in X_i, \tag{39}$$

$$[\bar{D}^i\ \bar{W}^i]^T = E_i z, \tag{40}$$

Please cite this article as: Li, S, Liu, R, Gao, Z. and Yang, L (2021) Integrated train dwell time regulation and train speed profile generation for automatic train operations on high-density metro lines: A distributed optimal control method. Transportation Research Part B. 148, 82-105. https://doi.org/10.1016/j.trb.2021.04.009

where $f_i(\bar{D}^i, L^i, \bar{W}^i, x_k^i, p^i, u_s^i, y_k^i, \delta^i) = \sum_{(i,j)|j\in N_{i,h}} [\alpha(D_j^i - D_j^{i-1} - H)^2 + \beta(m_{1i}\sum_{k=1}^{m} y_{j,k}^i e_{j,k}^i + m_{2i}\sum_{k=1}^{m} x_{j,k}^i e_{j,k}^i)]$. The constraints set X_i includes all constraints (22)-(29) for each train i and its neighbor $i-1$. In particular, the coupling constraints (22)-(25) are also included in the set X_i. E_i is a matrix that picks out components of global variable z that matches components of the local variable $\bar{D}^i$ and $\bar{W}^i$. The mapping from local variable indices of $[\bar{D}^i\ \bar{W}^i]$ into global variable index of z can be further written as $g = G(i,j)$ which means that the j-th component of variable $[\bar{D}^i, \bar{W}^i]$ corresponds to global variable component z_g. It is obvious that the problem (38) has a separate cost function in variables $(\bar{D}_j^i, L_j^i, \bar{W}_j^i, y_{j,k}^i, {u_s}_j^i)$ with only coupling equality constraint (40), which enforces consistency of local variable copies.

3.1.2. Dualization and decomposition

ADMM is a method to combine the robustness of the standard dual decomposition with multipliers. By denoting $\bar{z}_i = E_i z$, the augmented Lagrangian for the optimization problem (38) is given as

$$\begin{aligned} &L_\rho(D, L, W, x, p, u, y, z, \lambda) \\ &= \sum_{i\in M}\left[f_i(\bar{D}^i, L^i, \bar{W}^i, x_k^i, p^i, u_s^i, y_k^i, \delta^i) + \lambda_i^T([\bar{D}^i\ \bar{W}^i]^T - \bar{z}_i) + \frac{\sigma}{2}\|[\bar{D}^i\ \bar{W}^i]^T - \bar{z}_i\|_2^2\right], \end{aligned} \tag{41}$$

where λ_i are Lagrange multipliers and $\sigma > 0$ is the corresponding penalty parameter.

For (41), the alternating direction method of multipliers algorithm includes the following three step iterations.

(1) The update of $(\bar{D}^i, L^i, \bar{W}^i, x_k^i, p^i, u_s^i, y_k^i, \delta^i)$.

$$\begin{aligned} &(\bar{D}^i, L^i, \bar{W}^i, x_k^i, p^i, u_s^i, y_k^i, \delta^i) \\ &= \arg\min_{(\bar{D}^i, L^i, \bar{W}^i, x_k^i, p^i, u_s^i, y_k^i, \delta^i)\in X_i} f_i(\bar{D}^i, L^i, \bar{W}^i, x_k^i, p^i, u_s^i, y_k^i, \delta^i) + \lambda_i^T(l)([\bar{D}^i\ \bar{W}^i]^T - \bar{z}_i(l)) \\ &\quad + \frac{\sigma}{2}\|[\bar{D}^i\ \bar{W}^i]^T - \bar{z}_i(l)\|_2^2 \\ &= \arg\min_{(\bar{D}^i, L^i, \bar{W}^i, x_k^i, p^i, u_s^i, y_k^i, \delta^i)\in X_i} f_i(\bar{D}^i, L^i, \bar{W}^i, x_k^i, p^i, u_s^i, y_k^i, \delta^i) + \lambda_i^T(l)[\bar{D}^i\ \bar{W}^i]^T \\ &\quad + \frac{\sigma}{2}\|[\bar{D}^i\ \bar{W}^i]^T - \bar{z}_i(l)\|_2^2. \end{aligned} \tag{42}$$

(2) The update of z.

$$\begin{aligned} &z(l+1) = \arg\min_z L_\rho(\bar{D}(l+1), \bar{W}(l+1), z, \lambda(l)) \\ &= \arg\min_z \sum_{i\in M}\big[f_i(\bar{D}^i(l+1), L^i(l+1), \bar{W}^i(l+1), y_k^i(l+1), u_s^i(l+1)) \\ &\qquad +\lambda_i(l)^T([\bar{D}^i(l+1)\ \bar{W}^i(l+1)]^T - \bar{z}_i) + \frac{\sigma}{2}\|[\bar{D}^i(l+1)\ \bar{W}^i(l+1)]^T - \bar{z}_i\|_2^2\Big] \\ &= \arg\min_z \sum_{i\in M}\left[-\lambda_i(l)^T\bar{z}_i + \frac{\sigma}{2}\|[\bar{D}^i(l+1)\ \bar{W}^i(l+1)]^T - \bar{z}_i\|_2^2\right]. \end{aligned} \tag{43}$$

(3) The update of λ_i.

$$\lambda_i(l+1) = \lambda_i(l) + \sigma([\bar{D}^i(l+1)\ \bar{W}^i(l+1)]^T - \bar{z}_i(l+1)). \tag{44}$$

For the above algorithm, the $(\bar{D}^i, L^i, \bar{W}^i, x_k^i, p^i, u_s^i, y_k^i, \delta^i)$-updates and λ_i-updates can be carried out independently in parallel for each train i. However, the z-updates are not independently in parallel for each

Please cite this article as: Li, S, Liu, R, Gao, Z. and Yang, L (2021) Integrated train dwell time regulation and train speed profile generation for automatic train operations on high-density metro lines: A distributed optimal control method. Transportation Research Part B. 148, 82-105. https://doi.org/10.1016/j.trb.2021.04.009

train i, which is thereby not completely distributed. Moreover, based on the special form of the coupling structure for train communications, the z-updates can be decoupled across the components of z, which is given by the following theorem.

Theorem 3.1. *The global variable z update can be further decomposed for the update $\bar{z}_i$ of each train i as follows: for the component z_g of variable $\bar{z}_i$ of each train i, we have the following closed-form solution*

$$z_g(l+1) = \frac{1}{2} \sum_{G(i,j)=g} [\bar{D}^i(l+1)\ \bar{W}^i(l+1)]_j, \tag{45}$$

where $[\bar{D}^i(l+1)\ \bar{W}^i(l+1)]_j$ under $G(i,j) = g$ denotes the j-th components of $[\bar{D}^i(l+1)\ \bar{W}^i(l+1)]$ that map to the g-th component of z.

Proof. See Appendix A. □

With the result in Theorem 3.1, the $(\bar{D}^i, L^i, \bar{W}^i, x_k^i, p^i, u_s^i, y_k^i, \delta^i)$-updates, $\bar{z}_i$-updates and λ_i-updates can be calculated independently in parallel for each train i, which realize the distributed control for each train with the communication only with its neighboring trains.

3.2. Heuristic approach for the nonconvex constraints

Due to the integrality constraints of binary variables y_k^i and δ^i, the formulated optimization model (38) is nonconvex and discontinuous, in which the convergence of the standard ADMM algorithm is not guaranteed. To enhance the algorithm performance, the ADMM-based heuristic approach is developed to obtain high-quality solutions. To solve the linear quadratic mixed integer programming problem, the methods such as branch-and-bound and branch-and-cut are usually used to find global solutions. Unfortunately, these methods have non-polynomial worst-case run time, which are often burdensome for the use of embedded optimization in practice. In the algorithm runtime, these methods also suffer from a large variance. In the embedded applications, the computational resource is limited and the problem solution is required to be found in a very small time. Therefore, the method to find the global solution is usually not favorable, since its large variance in the computing runtime cannot be tolerated.

To realize the embedded application of dynamic train regulation and speed profile generation, a simple and computationally efficient heuristic based on the relax-round-polish process is designed to find approximate solutions to the problem (38) quickly. The solution process is to solve the continuous relaxed convex problem by the standard ADMM and find an integer feasible solution in the neighborhood of the continuous-relaxed convex solution. The computationally efficient heuristic includes three iteration steps: convex proximal, projection and polishing, which are presented as follows.

(1) Convex proximal step (relax)

In this step, we first relax the binary variables y_k^i and δ^i into a convex constraint set $[0, 1]$. Then the convex relaxation of (38) is formulated as follows

$$(\bar{D}^i, L^i, \bar{W}^i, x_k^i, p^i, u_s^i, \bar{y}_k^i, \bar{\delta}^i) = \arg\min \sum_{i \in M} f_i(\bar{D}^i, L^i, \bar{W}^i, x_k^i, p^i, u_s^i, y_k^i, \delta^i) \tag{46}$$

where y_k^i and δ^i belong to a convex constraint set $[0, 1]$. The constraints for other variables are the same to the problem (38). This step can be solved by the standard ADMM iterations (42)-(44). The convergence of the standard ADMM has been proven by (Boyd et al., 2011) for the problem formulated with convex quadratic objective function and linear constraints.

Please cite this article as: Li, S, Liu, R, Gao, Z. and Yang, L (2021) Integrated train dwell time regulation and train speed profile generation for automatic train operations on high-density metro lines: A distributed optimal control method. Transportation Research Part B. 148, 82-105. https://doi.org/10.1016/j.trb.2021.04.009

(2) Projection step (round)

The (nonconvex) projection step is formulated by

$$[\hat{y}_k^i, \hat{\delta}^i] = \Pi(\bar{y}_k^i, \bar{\delta}^i), \tag{47}$$

where Π denotes Euclidean projection onto the binary set $\{0, 1\}$.

(3) Polishing step (polish)

Find the solutions to the problem (38), by solving the polishing problem with restriction of $\hat{y}_k^i$ and $\hat{\delta}^i$ as follows

$$(\bar{D}^i, L^i, \bar{W}^i, x_k^i, p^i, u_s^i, y_k^i, \bar{\delta}^i) = \arg\min \sum_{i \in M} f_i(\bar{D}^i, L^i, \bar{W}^i, x_k^i, p^i, u_s^i, \hat{y}_k^i, \hat{\delta}^i). \tag{48}$$

This step can also be solved by the standard ADMM iterations (42)-(44).

With this process, the algorithm remains a complete distributed control algorithm in the framework of ADMM iterations, where each train makes its control decision, in the sense that the binary variables y_k^i and δ^i are the local variables for each train, which are not the global variables. Moreover, we can get a lower bound on the optimal value of the problem (38) in the first step, an upper bound in the polishing step, and a feasible solution if polishing is successful. To improve the success of the polishing, we can further introduce randomization by replacing the round step with $[\hat{y}_k^i, \hat{\delta}^i] = \Pi(\bar{y}_k^i + w_k^i, \bar{\delta}^i + w^i)$, where w_k^i and w^i are random vectors. We can repeat the heuristic with K different random vectors and obtain a set of K candidate solutions. The best among these K candidates can be taken as the final solution.

3.3. The whole distributed optimal control algorithm

With the computationally efficient relax-round-polish heuristic algorithm, we can finally formulate an ADMM-based heuristic algorithm for the whole problem, where the standard ADMM is to achieve the distributed control for each train, while the heuristic step is to deal with the integrality constraints of binary variables to achieve the embedded control. Under the rolling horizon scheme, dualization, decomposition and linearization, the whole distributed optimal control algorithm for dynamic train regulation and speed profile generation is summarized as follows.

Algorithm 3.1. *ADMM-based heuristic algorithm for dynamic train regulation and speed profile generation.*

Step 1. *At decision interval h, get the available information of train departure time, passenger load and left passenger at station as $\{L_j^i, W_j^i, D_j^i | (L_j^i, W_j^i, D_j^i) \in A_h\}$.*

Step 2. *Given a predicted horizon T, formulate the optimal control problem (38) with constraints (39)-(40).*

Step 3. *Solve the optimal control problem (38) in a distributed manner as follows.*

For each train i in parallel:

(1) The convex proximal step. By relaxing the binary variables y_k^i and δ^i into a convex constraint set $[0, 1]$, calculate as the following standard ADMM iterations

repeat *Initialize $l = 1$, $\lambda_i(1) = 0$, $z_i(1) = 0$.*

1) Calculate

$$\begin{aligned}&(\bar{D}^i(l+1), L^i(l+1), \bar{W}^i(l+1), x_k^i(l+1), p^i(l+1), u_s^i(l+1), \bar{y}_k^i(l+1), \bar{\delta}^i(l+1)) \\ &= \arg\ \min f_i(\bar{D}^i, L^i, \bar{W}^i, x_k^i, p^i, u_s^i, y_k^i, \delta^i) + \lambda_i^T(l)[\bar{D}^i\ \bar{W}^i]^T + \frac{\sigma}{2}\|[\bar{D}^i\ \bar{W}^i]^T - \bar{z}_i(l)\|_2^2.\end{aligned} \tag{49}$$

Please cite this article as: Li, S, Liu, R, Gao, Z. and Yang, L (2021) Integrated train dwell time regulation and train speed profile generation for automatic train operations on high-density metro lines: A distributed optimal control method. Transportation Research Part B. 148, 82-105. https://doi.org/10.1016/j.trb.2021.04.009

by a linear quadratic programming algorithm.

2) According to $\bar{D}_j^i = [D_j^i, D_j^{i-1}]$ *and* $\bar{W}_j^i = [W_j^i, W_j^{i-1}]$*, communicate* D_j^i *and* $\bar{W}_j^i$ *to all the neighbors* $j : j \in N_i$*.*

3) Calculate the variable $\bar{z}_i$ *for each train* i *as follows.*

$$z_g(l+1) = \frac{1}{2} \sum_{G(i,j)=g} [\bar{D}^i(l+1)\ \bar{W}^i(l+1)]_j \tag{50}$$

where z_g *is the component of variable* $\bar{z}_i$ *for each train* i

4) Calculate the Lagrangian multiplier for each train i*:*

$$\lambda_i(l+1) = \lambda_i(l) + \sigma([\bar{D}^i(l+1)\ \bar{W}^i(l+1)] - \bar{z}_i(l+1)). \tag{51}$$

until *The interaction balance constraints are satisfied, or the termination condition is reached.*

(2) The nonconvex projection step.

$$[\hat{y}_k^i, \hat{\delta}^i] = \Pi(\bar{y}_k^i, \bar{\delta}^i), \tag{52}$$

where Π *denotes Euclidean projection onto the binary set* $\{0, 1\}$*.*

(3) The polishing step. Find the solutions to the problem (38), by solving the polishing problem with restriction of $\hat{y}_k^i$ *and* $\hat{\delta}^i$ *as following standard ADMM iterations*

$$\begin{aligned}&(\bar{D}^i(l+1), L^i(l+1), \bar{W}^i(l+1), x_k^i(l+1), p^i(l+1), u_s^i(l+1), y_k^i(l+1), \bar{\delta}^i(l+1)) \\ &= \arg\ \min f_i(\bar{D}^i, L^i, \bar{W}^i, x_k^i, p^i, u_s^i, \hat{y}_k^i, \hat{\delta}^i) + \lambda_i^T(l)[\bar{D}^i\ \bar{W}^i]^T + \frac{\sigma}{2}\|[\bar{D}^i\ \bar{W}^i]^T - \bar{z}_i(l)\|_2^2.\end{aligned} \tag{53}$$

$$z_g(l+1) = \frac{1}{2} \sum_{G(i,j)=g} [\bar{D}^i(l+1)\ \bar{W}^i(l+1)]_j. \tag{54}$$

$$\lambda_i(l+1) = \lambda_i(l) + \sigma([\bar{D}^i(l+1)\ \bar{W}^i(l+1)] - \bar{z}_i(l+1)). \tag{55}$$

Step 4. *Obtain the optimal dynamic train control and speed profile and implement it to each train* i *at the decision interval* h*.*

Step 5. *At the next decision interval* $h+1$*, measure the new values of train departure time, passenger load and left passenger at station, repeat Steps 1-4 until the end time horizon.*

Figure 5 illustrates the proposed distributed and embedded optimal control algorithm 3.1 for the dynamic generation of train control and speed profile. This algorithm breaks a complex optimal control problem with coupling constraints into many smaller optimal control problems that can be computed in parallel. At each iteration step of the algorithm, only a relatively small linear quadratic programming regarding each train needs to be solved, which can be done very fast using the existing optimization tool box. The algorithm therefore satisfies the real-time requirement for dynamic train control and speed regulation generation that needs to be calculated in three seconds in practice. In this algorithm, we assume that all the exchanges are perfect between the trains, i.e., there is no information or data loss for the communications among trains. Additionally, it should be noted that, if a new train enters the considered system or the existing train leaves this system, the algorithm involving the new train or the leaving train only needs to be modified, which indicates a good robustness performance of the proposed distributed and embedded optimal control algorithm with respect to the dynamic structure of multiple trains movement. This inherent modularity simplifies

Please cite this article as: Li, S, Liu, R, Gao, Z. and Yang, L (2021) Integrated train dwell time regulation and train speed profile generation for automatic train operations on high-density metro lines: A distributed optimal control method. Transportation Research Part B. 148, 82-105. https://doi.org/10.1016/j.trb.2021.04.009

the system maintenance and allows further expansions for the optimal control system. Furthermore, the modularity generates more robustness by the comparison with a centralized optimal controller. The failure or damage for one sub-system does not necessarily affect the whole system control design, as such, the distributed control method has greater tolerance and resilience to the failures.

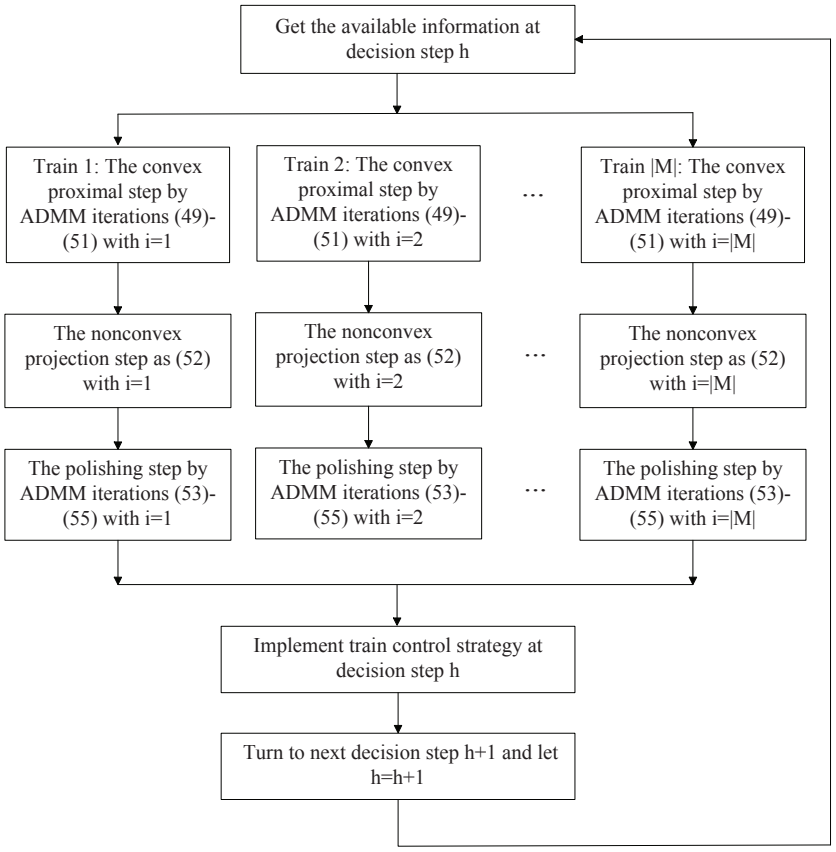

Figure 5. The flowchart of ADMM-based heuristic algorithm.

4. Numerical simulations

4.1. Parameter Settings

In this section, numerical simulations are implemented to illustrate the effectiveness of the proposed distributed optimal control for train regulation and speed profile generation. The detailed implementation and testing of the proposed model and methods are firstly introduced to Beijing Changping metro line. Further tests on the computational performance of the proposed distributed optimization algorithm are conducted on five additional lines in Beijing metro.

First, the Changping line is shown in Figure 6. There are 12 stations on the line, where station Xi' Erqi and Changping Xishankou are two terminal stations. The operational 'up' direction is from Xi' Erqi to Changping Xishankou, while the 'down' direction is from Changping Xishankou to Xi' Erqi. Combining the up and down directions, the line can be reformulated as a loop structure with a total of 22 stations.

Please cite this article as: Li, S, Liu, R, Gao, Z. and Yang, L (2021) Integrated train dwell time regulation and train speed profile generation for automatic train operations on high-density metro lines: A distributed optimal control method. Transportation Research Part B. 148, 82-105. https://doi.org/10.1016/j.trb.2021.04.009

We choose the metro line operation during morning hours from 7 : 00 to 10 : 00 and there are 22 trains operating on the line over this time period. The scheduled headway is $H = 240$s. The minimum headway is $H_{\min} = 200$s. In addition, the maximum train capacity is $l_{\max} = 1500$, the mass for each train without passengers is $m_{1i} = 224$t, the average mass per passenger is assumed 60kg, the maximum capacity of the platform is $W_{\max} = 500$, the maximum allowable train dwell time adjustment $\bar{u}_s = 20$s, and the delay rate ρ is given as 0.02.

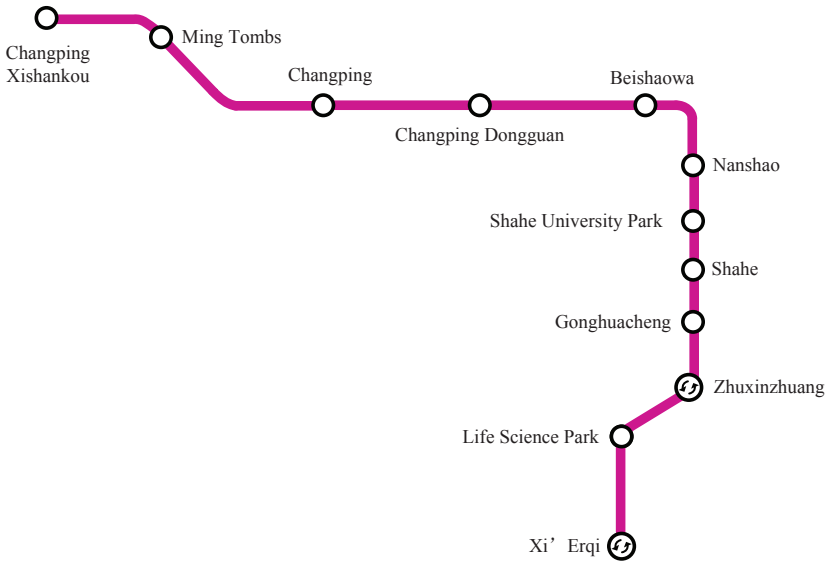

Figure 6. The map of Beijing Changping metro line.

Table 3. The nominal running time and energy consumption per mass.

Station	Index j	NRT(s)	NECP(kwh/t)	Index j	NRT(s)	NECP(kwh/t)
Xi' Erqi	1	277.4	0.1830	-	314.6	0.1250
Life Science Park	2	158.4	0.1161	22	159	0.1295
Zhuxinzhuang	3	213.8	0.1518	21	211.8	0.1473
Gonghuacheng	4	127.2	0.1071	20	126.2	0.1161
Shahe	5	124	0.1250	19	128.2	0.1161
Shahe University Park	6	264	0.1786	18	278.8	0.2321
Nanshao	7	138.8	0.1339	17	135.6	0.1071
Beishaowa	8	108.4	0.1071	16	111.4	0.0982
Changping Dongguan	9	139.6	0.1295	15	142.6	0.1607
Changping	10	181.8	0.2366	14	180.8	0.1473
Ming Tombs	11	98	0.1071	13	99.2	0.0804
Changping Xishankou	12	-	-	-	-	-

According to the practical operating data of the Changping Line, the nominal train running time (NRT) and energy consumption per mass (NECP) corresponding to the nominal speed profile is given in Table

Please cite this article as: Li, S, Liu, R, Gao, Z. and Yang, L (2021) Integrated train dwell time regulation and train speed profile generation for automatic train operations on high-density metro lines: A distributed optimal control method. Transportation Research Part B. 148, 82-105. https://doi.org/10.1016/j.trb.2021.04.009

3. There are five speed profiles stored for each inter-station (including the nominal speed profile), each corresponds to a running time and energy consumption. Table 4 shows the running time (RT) and energy consumption per mass (ECP) associated with all the five stored speed profiles for the stations from Xi' Erqi to Shahe University Park (Station 1 to 6). It can be seen that higher RT leads to lower ECP.

The variable passenger alighting and arrival rates are drawn from the automatic fare collection (AFC) data, which provides the passenger arrival rate and alighting rates for each station. AFC data from a typical weekday of 2017 and during 7 : 00 and 10 : 00 are processed. In particular, the passenger entering number for the 5-minute period between 7 : 00 to 8 : 30 of Station 19-22 are plotted in Figure 7, and the data for the arrival rate (ER) and alighting rate (AR) for each station during 7 : 00 to 7 : 05 are given as Table 5, which show variations of passenger arrival and alighting flows by station and by time. The proposed distributed and embedded optimal control algorithm is conducted by the MATLAB R2016a on a PC (2.6-GHz processor speed and 16-GB memory size). At each iteration step, the formulated quadratic convex programming problem is effectively solved by the quadprog function in the MATLAB optimization tool box that provides an interior point algorithm to rapidly calculate the optimal value.

Table 4. The different speed mode from station 1 to 6.

Station j		Mode 1	Mode 2	Mode 3	Mode 4	Mode 5
1	RT(s)	258.4	268.8	277.4	291	312.6
	ECP(kwh/t)	0.2277	0.2054	0.1830	0.1518	0.1161
2	RT(s)	147.3	155.8	158.4	163.2	167.4
	ECP(kwh/t)	0.1652	0.1429	0.1161	0.0938	0.0804
3	RT(s)	204	210	213.8	227	242.4
	ECP(kwh/t)	0.1875	0.1696	0.1518	0.0982	0.0893
4	RT(s)	117.4	124.4	127.2	131.4	134.6
	ECP(kwh/t)	0.1607	0.1295	0.1071	0.0938	0.0893
5	RT(s)	120.2	123.2	124	131.2	135.2
	ECP(kwh/t)	0.1563	0.1384	0.1250	0.1071	0.0938
6	RT(s)	254.6	259.6	264	267.2	280.6
	ECP(kwh/t)	0.2455	0.2143	0.1786	0.1786	0.1563

Please cite this article as: Li, S, Liu, R, Gao, Z. and Yang, L (2021) Integrated train dwell time regulation and train speed profile generation for automatic train operations on high-density metro lines: A distributed optimal control method. Transportation Research Part B. 148, 82-105. https://doi.org/10.1016/j.trb.2021.04.009

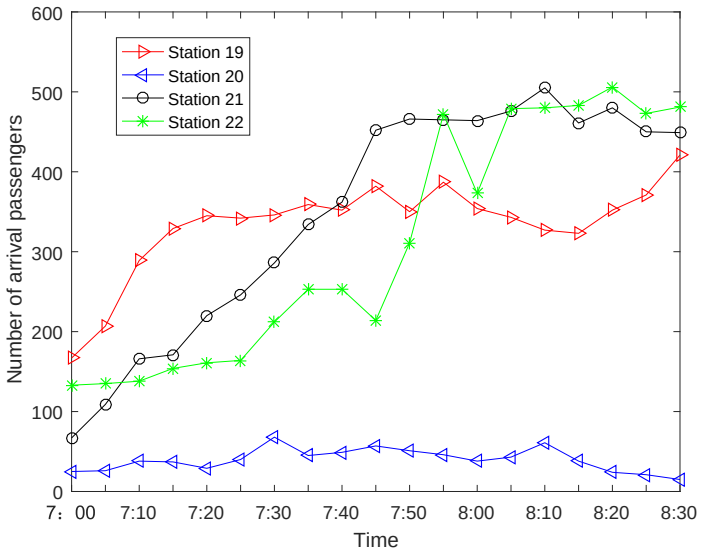

Figure 7. Number of arrival passengers in 5-minute intervals.

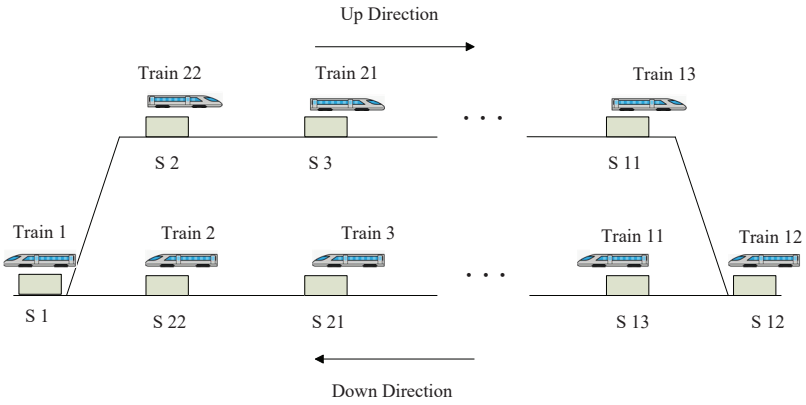

Figure 8. The loop structure and train operations at time 7 : 00.

Please cite this article as: Li, S, Liu, R, Gao, Z. and Yang, L (2021) Integrated train dwell time regulation and train speed profile generation for automatic train operations on high-density metro lines: A distributed optimal control method. Transportation Research Part B. 148, 82-105. https://doi.org/10.1016/j.trb.2021.04.009

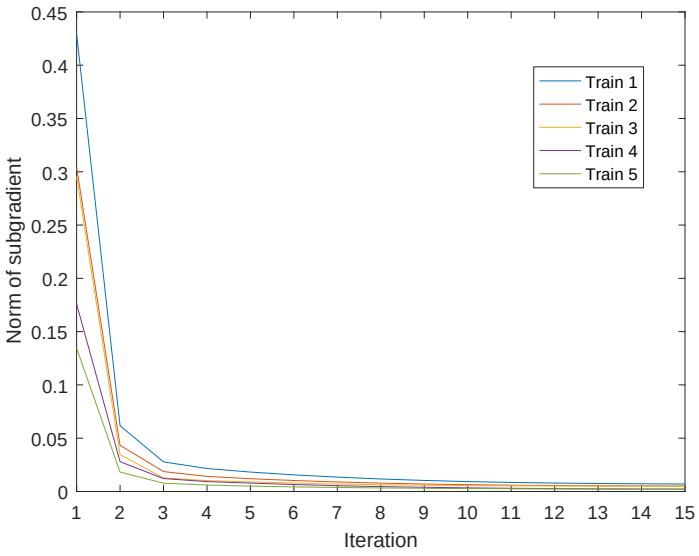

Figure 9. The convergence of the computation process.

Table 5. The average passenger arrival rate (ER) and alighting rate (AR) during time 7 : 00 to 7 : 05.

Station j	ER(passenger/s)	AR	Station j	ER(passenger/s)	AR
1	0.1794	1	12	0.1111	1
2	0.0689	0.17	13	0.0722	0.05
3	0.0567	0.12	14	0.6111	0.13
4	0.0233	0.03	15	0.1556	0.11
5	0.0833	0.40	16	0.1111	0.04
6	0.1094	0.16	17	0.2500	0.07
7	0.0744	0.14	18	0.4444	0.02
8	0.0183	0.04	19	0.5556	0.10
9	0.0750	0.18	20	0.0833	0.01
10	0.0372	0.8	21	0.2222	0.11
11	0.0122	0.6	22	0.4444	0.07

The reformulated loop structure for the Beijing Changping metro line with the up and down directions is plotted in Figure 8. Without loss of generality, based on this loop structure and operating directions, we consider that from time 7 : 00, train 1 is departing from station 1(S 1), train 2 is departing from station 22(S 22), ..., and train 22 is departing from station 2(S 2), which are clearly shown in Figure 8. For the proposed ADMM algorithm, we set the algorithm parameters $\sigma = 10$. Under the given algorithm parameters, to illustrate the convergence speed for the proposed algorithm clearly, the evolution of the norm of the subgradients for trains 1-5 in the computation process is plotted in Figure 9. It shows that the best feasible solution can be obtained after 12 iterations. Consider that the maximum computation time for each iteration is only 0.01s. The best feasible solution at each decision stage can be obtained within 1s, which satisfies the real-time requirement in practice. Additionally, by comparison, the computation time for the traditional centralized train regulation algorithm with the IBM ILOG CPLEX 12.5.0 solver is up to

Please cite this article as: Li, S, Liu, R, Gao, Z. and Yang, L (2021) Integrated train dwell time regulation and train speed profile generation for automatic train operations on high-density metro lines: A distributed optimal control method. Transportation Research Part B. 148, 82-105. https://doi.org/10.1016/j.trb.2021.04.009

8.7s, along with the communication delay time, which is more than 9s. Therefore, the proposed distributed algorithm is more superior for the practical applications.

Table 6. The computational performance of different metro lines.

Metro line	Number of stations	Number of trains	Iteration number	CPU time (s)
Line 16	18	18	10	0.10
Changping Line	22	22	12	0.12
Line 9	24	23	12	0.12
Yizhuang Line	26	26	14	0.14
Line 13	32	31	17	0.17
Line 5	44	42	21	0.21

To further test the computational performance of the proposed distributed optimal control algorithm, we conduct experiments on five other Beijing metro lines with different numbers of stations. The same operation period between 7 : 00 and 10 : 00 is considered for these lines. Passenger alighting and arrival rates at stations along these lines are set to empirically derived passenger demand. There are five pre-generated speed profiles for each inter-station segment of each line. Other parameters such as the scheduled headway, the mass for each train and the maximum train capacity are assumed to be the same for all five lines. The total number of stations (in a looped network) and operating trains for each line (including the Changping Line) are listed in Table 6. Also listed in Table 6 are the number of iterations and the CPU time it takes to reach the best feasible solution for each line. It is understandable that the number of iterations increases with increasing numbers of stations and trains, because the distributed optimal control algorithm (Algorithm 3.1) calculates the optimal departure time of each train at each stopping station. The computation time for each iteration is 0.01s, which is however not affected by the number of the stations and trains, as the formulated linear quadratic programming problem is solved for each train in each iteration. Thus, the total computation time to reach the best feasible solution also increases with the increasing number of stations and trains on the line. The six lines tested are representative of Beijing Metro lines, in terms of their number of stations. Overall, we can see from Table 6 that the best feasible solution at each decision stage can be comfortably obtained within 1s, indicating that our proposed distributed optimal control algorithm is applicable in practical applications.

4.2. The performance of different control strategies

In this section, under the same initial train delays and real-time disturbances, we compare the following three control strategies to validate the effectiveness of the proposed distributed train regulation and speed profile generation strategy in this study. The considered time horizon is chosen as $T = 8$.

(1) Case 1: Nominal control strategy (NCS). In this case, the speed profile is generated based on the nominal speed profile, and the dwell time adjustment is applied based on the safety headway. NCS is a benchmark for purposes of comparison.

(2) Case 2: Local heuristic strategy (LHS). This strategy is usually adopted in the practical train operation process, where each train generates the speed profile only based on its own state feedback information and with the objective to the reduction as much delay as possible.

Please cite this article as: Li, S, Liu, R, Gao, Z. and Yang, L (2021) Integrated train dwell time regulation and train speed profile generation for automatic train operations on high-density metro lines: A distributed optimal control method. Transportation Research Part B. 148, 82-105. https://doi.org/10.1016/j.trb.2021.04.009

(3) Case 3: The proposed dynamic generation strategy (DGS). This case is based on the algorithm 3.1 with global information and is solved in a distributed control framework, where the predictive stage is chosen as 3. To achieve the headway regularity and energy efficiency, the weights in the objective are chosen as $(\alpha, \beta) = (1, 10)$.

Under each of the three control strategies, we calculate the corresponding headway deviations and energy consumptions for each train with the same given initial train delays and disturbances. The total headway deviations for each train i over the considered time horizon under these different cases are plotted in Figure 10. It is clearly shown that, the total headway deviations for most trains under case 1 are larger than those under cases 2 and 3, suggesting that the local heuristic strategy of case 2 and the proposed dynamic generation strategy of case 3 can both reduce the headway deviations. Moreover, we can also observe that total headway deviations for most trains of case 2 are larger than that of case 3, which indicates that the proposed dynamic generation strategy by the information interaction between trains can achieve less headway deviations than the local heuristic strategy. Specifically, the total headway deviations for all the trains 1-22 over the considered time horizon are calculated as summarized in the columns 2-4 of Table 7, where the average headway deviations in cases 1-3 are 79.5, 40.3 and 28.8 respectively. The local heuristic strategy (case 2) reduces the average headway deviation by 49.3% compared to the nominal control strategy, while the proposed dynamic generation strategy is reduced by 63.7%. Under the proposed dynamic generation strategy (case 3), the average headway deviation is further reduced by 14.4% compared to the local heuristic strategy, which effectively improves the headway regularity of the metro line system from a view of system optimization.

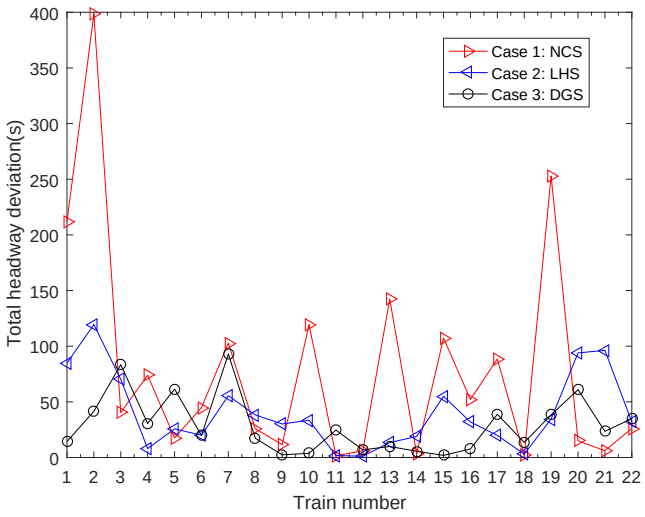

Figure 10. The total headway deviations for each train under different cases.

Please cite this article as: Li, S, Liu, R, Gao, Z. and Yang, L (2021) Integrated train dwell time regulation and train speed profile generation for automatic train operations on high-density metro lines: A distributed optimal control method. Transportation Research Part B. 148, 82-105. https://doi.org/10.1016/j.trb.2021.04.009

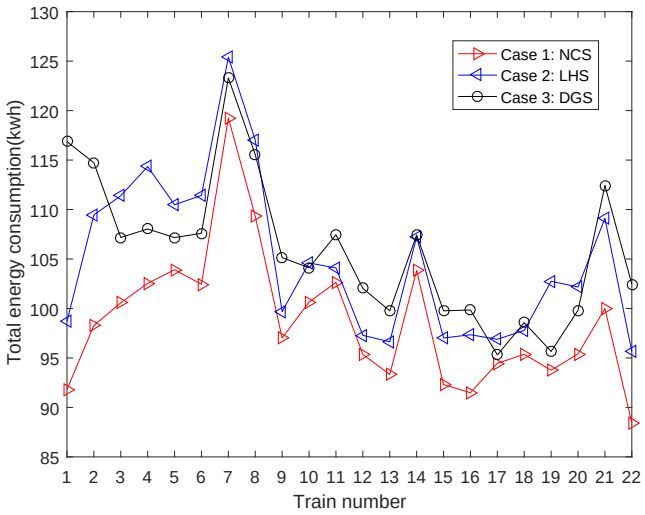

Figure 11. The total energy consumptions for each train under different cases.

Table 7: The comparison results of headway deviations(HD) (unit: s) and energy consumptions(EC) (unit: kwh) in cases 1-3.

Train	Case 1(HD)	Case 2(HD)	Case 3(HD)	Case 1(EC)	Case 2(EC)	Case 3(EC)
1	212.0	84.8	14.3	91.8	98.7	116.8
2	398.2	119.4	41.5	98.2	109.4	114.7
3	40.3	70.1	83.4	100.5	111.3	107.1
4	73.9	7.9	30.5	102.5	114.3	108.0
5	17.6	25.7	61.4	103.9	110.4	107.1
6	44.7	19.9	19.8	102.4	111.4	107.6
7	102.7	55.5	92.9	119.2	125.4	123.3
8	25.9	38.2	17.3	109.3	117.0	115.5
9	11.5	30.1	2.4	97.0	99.6	105.1
10	119.3	33.4	3.7	100.6	104.6	104.1
11	1.4	1.7	24.6	102.6	104.0	107.4
12	6.1	1.1	6.8	95.3	97.2	102.0
13	142.1	13.4	9.8	93.3	96.6	99.7
14	3.4	18.9	5.5	103.8	107.2	107.4
15	107.2	54.9	1.9	92.3	97.0	99.7
16	52.1	31.9	7.6	91.4	97.3	99.8
17	88.5	19.8	38.8	94.4	96.8	95.3
18	2.1	3.0	13.5	95.3	97.7	98.5
19	252.9	34.5	38.4	93.7	102.7	95.6
20	15.0	93.9	60.8	95.4	102.1	99.8
21	6.0	96.2	23.4	99.9	109.1	112.4
22	26.1	31.9	34.9	88.4	95.6	102.4
Ave.	79.5	40.3	28.8	98.7	104.8	105.9

Please cite this article as: Li, S, Liu, R, Gao, Z. and Yang, L (2021) Integrated train dwell time regulation and train speed profile generation for automatic train operations on high-density metro lines: A distributed optimal control method. Transportation Research Part B. 148, 82-105. https://doi.org/10.1016/j.trb.2021.04.009

The total energy consumptions for each train i over the considered time horizon under these different cases are plotted in Figure 11. We can observe that, case 2 and case 3 generate more energy consumptions than case 1 due to the speed control strategy that has been adopted to reduce the headway deviations. It appears therefore the reductions in headway deviation will bring increases in energy consumptions. Between case 2 and case 3, their effect on energy consumption vary by trains (Fig. 10): on some of the trains, the energy consumption under case 3 is lower than that under case 2, while on other trains, the opposite is true. Specifically, the total energy consumptions for all the trains 1-22 over the considered time horizon are calculated as summarized in the columns 5-7 of Table 7. We can observe that the average energy consumptions for cases 2 and 3 are 104.8 and 105.9, respectively, and the difference between these two cases is very small. Therefore, by combining the headway deviation results, we can obtain that the proposed dynamic generation strategy not only further reduces the average headway deviations, but also keeps the similar average energy consumptions, compared to the local heuristic strategy. The objective value under the proposed distributed optimal control algorithm is obtained as 2.51×10^6, which can be regarded as an upper bound on the formulated optimal control problem in the rolling horizon scheme. A lower bound on the optimal value of the corresponding formulated optimal control problem is calculated as 2.18×10^6 in the convex proximal step by relaxing the binary variables. Therefore, the gap between the upper bound (obtained solutions) and lower bound of the formulated optimal control problem is less than 13.2%. This suggests that the proposed ADMM-based heuristic algorithm is able to obtain an accepted high-quality solution in a relatively short time (within 1s), especially for the nonlinear optimal control problem.

4.3. Robustness of the proposed distributed optimal control method

In actual metro line operation, the real time data for passenger arrival rate λ_j^i and train running time and dwell time disturbance $\bar{w}_j^i$ could be inaccurate or incomplete in practice. Therefore, the robustness of the proposed distributed optimal control method is important. Based on these considerations, in this section, we present experiments to investigate the robustness of the proposed distributed optimal control method to the passenger demand and disturbances uncertainty parameters with errors.

Table 8: Computation results under uncertain passenger arrival rates (case 1-5) and uncertain train running time disturbances (case 6-10).

Case	AHD(s)	AEC(kwh)	Case	AHD(s)	AEC(kwh)
1	25.22	105.34	6	28.23	105.70
2	25.59	105.31	7	26.61	105.65
3	25.58	105.68	8	28.65	105.98
4	25.15	105.65	9	26.34	106.03
5	25.03	105.35	10	28.83	106.09
Ave.	25.31	105.47	Ave.	27.73	105.89
Std.	0.26	0.18	Std.	1.17	0.20

First, we conduct simulation experiments to evaluate the robustness of the proposed control method to demand uncertainty. Keeping the train running time and dwell time disturbances, we allow the passenger arrival rates λ_j^i to vary randomly over a range of $[-0.02, 0.02]$ passenger/s to the mean values for each station and each optimal decision time period. The proposed distributed optimal control method is run five times, with five different random number seeds, and the average headway deviations(AHD) and energy

consumptions(AEC) for all the trains along the considered time horizon over the five cases (case 1-5), and their standard deviations, are calculated and summarized in columns 1-3 of Table 8. We can observe that with the fluctuations in passenger arrival rates introduced, the deviations for the average headway deviations and the energy consumption are both very small, implying the robustness of the proposed method to the passenger demand uncertainty in reducing the headway deviation and energy consumption.

Second, for a given passenger demand, the robustness of the proposed method to train running time disturbance uncertainties are examined. In this experiment, we keep the passenger arrival rates as their default values. We test five cases where train running time disturbances are deviated randomly from their default values in the range $[-4, 4]$ s. The resulted average headway deviations (AHD) and energy consumptions (AEC) for all the trains along the considered time horizon under five cases (case 6-10) are calculated, and their standard deviations over the five cases are derived, and summarized in the columns 4-6 of Table 8. Again, the small standard deviations among the five test runs with fluctuations in train running time disturbances indicate the robustness of the proposed method to the uncertain running time disturbances in the reduction of the headway deviation and energy consumption. Moreover, we can also find that, the standard deviation of the energy consumption is smaller than that of the headway deviations under uncertain passenger demands and running time disturbances, which reveals that the proposed method is more robust in the energy consumption reduction, rather than in the headway deviation reduction with respect to passenger demands and running time disturbances uncertainties.

5. Conclusion

In this paper, a practical distributed optimal control is designed for real-time integrated train dwell time regulation and speed profile generation problem on automated high-density metro lines. A coupled model of passenger flow dynamics, train timetable dynamics and train speed profile generation is introduced to represent the interaction and relationships among them. A nonlinear optimal control model is formulated in a rolling horizon scheme to improve headway regularity and reduce the total energy consumptions with the updated information. Based on the coupled structure of multiple trains motion, an alternating direction method of multipliers (ADMM) based decomposition is designed to decompose the original optimal control problem into many sub-problems, one for each train, which can be computed in a distributed manner. Moreover, to address the nonconvexity issue, an ADMM-based heuristic algorithm combined with relax-round-polish process is proposed to find approximate solutions quickly for the embedded applications. The superiority of the distributed algorithm guarantees the flexibility and modularity of the optimal control problem.

The proposed coupled model explicitly captures the dynamics and interactions of train operations, passenger flow and speed control, and significantly enhances the authenticity and operability of real implementations. By coordinating in real-time dwell time change and speed profile regeneration, the proposed integrated strategy enables us to balance the tradeoff between the operation efficiency and the energy consumption in practical applications. The proposed distributed computation mechanism also has an advanced feature of the inherent modularity, which simplifies the expansions of the system and provides robustness in comparison with a centralized optimization method. Computational results are given to demonstrate the effectiveness and efficiency of the proposed model and algorithm. The best feasible solution at each decision stage can be obtained in less than 1s, well within the practical operational requirement. It is therefore particularly suited to on-line traffic regulation and can be directly implemented to existing ATO systems

Please cite this article as: Li, S, Liu, R, Gao, Z. and Yang, L (2021) Integrated train dwell time regulation and train speed profile generation for automatic train operations on high-density metro lines: A distributed optimal control method. Transportation Research Part B. 148, 82-105. https://doi.org/10.1016/j.trb.2021.04.009

for real-life practical operation of metro lines in response to the frequent disturbances. From the view of system optimization, the proposed integrated strategy outperforms the local heuristic strategy used in the practical train operation in terms of the reduction of headway deviations, while maintaining similar level of average energy consumptions. For different metro lines with the increasing number of the stations (in a looped network) from 18 to the maximum 44 for Beijing Metro, the computation times all fall within 1s, indicating strongly the applicability of the proposed method for practical implementations. The simulation experiments show that the proposed distributed optimal control method is robust to uncertain passenger demand and time disturbances parameters in reducing the headway deviation and energy consumption.

This study considers only passenger arrivals at platform. For overcrowded passenger arrivals to stations, a regular feature among morning peak travel in Beijing Metro, there is passenger flow control at station-entry. An interesting extension of the current study is to investigate the integrated train regulation, speed profile generation and passenger flow control strategy. A further research extension of the current research is to consider metro network with multiple intersecting lines and transfer connection constraints. There, each train needs the information of not only from its preceding train on the same line, but also trains from other lines at the transfer stations. This changes the information exchange relationship among trains and may require another decomposition method for the design of a distributed optimal control algorithm, which will be investigated in our future research.

Acknowledgements

This work is supported by the National Natural Science Foundation of China (Nos. 71890972, 71890970, 71771017) and by the Royal Academy of Engineering (Newton Fund UK–CIAPP\286 and TSPC1025).

Appendix A. Proof of Theorem 3.1

Proof. For the minimization of the right hand side of (43), by calculating its derivative with respect to each $\bar{z}_i$ and letting them equal to zero, we can get

$$\sum_{i=1}^{|M|}(-\frac{1}{\sigma}\lambda_i(l)+\bar{z}_i(l+1)-[\bar{D}^i(l+1)\ \bar{W}^i(l+1)])=0. \tag{56}$$

where $|M|$ represents the number of the set M.

Moreover, (56) is equivalent to

$$z_g(l+1)=\frac{1}{k_g}\sum_{G(i,j)=g}([\bar{D}^i(l+1)\ \bar{W}^i(l+1)]_j+\frac{1}{\sigma}(\lambda_i(l))_j), \tag{57}$$

where $G(i,j)=g$ denotes the j-th components of $[\bar{D}^i(l+1)\ \bar{W}^i(l+1)]$ that map to the g-th component of z, and k_g is the number of local variable entries that correspond to global variable entry z_g.

By averaging the λ_i-update as (44), we can obtain that

$$\frac{1}{k_g}\sum_{G(i,j)=g}(\lambda_i(l+1))_j=\frac{1}{k_g}\sum_{G(i,j)=g}((\lambda_i(l))_j+\sigma[\bar{D}^i(l+1)\ \bar{W}^i(l+1)]_j)-\sigma z_g(l+1). \tag{58}$$

Then, with the substitution of the expression $z_g(l+1)$ as (57) into (58), we can further get that

$$\sum_{G(i,j)=g}(\lambda_i(l+1))_j=0, \tag{59}$$

i.e., the local average value for the dual variables of each element z_g is zero after one iteration.

Based on the coupling structure that each train communicates with its ahead train, we can get that $k_g = 2$. Thus, the z-update step can be written in a simpler form as

$$z_g(l+1) = \frac{1}{2} \sum_{G(i,j)=g} [\bar{D}^i(l+1)\ \bar{W}^i(l+1)]_j. \tag{60}$$

The proof is complete. □

References

Bemporad, A., Morari, M., 1999. Control of systems integrating logic, dynamics, and constraints. Automatica 35 (3), 407–427.

Boyd, S., Parikh, N., Chu, E., Peleato, B., Eckstein, J., 2011. Distributed optimization and statistical learning via the alternating direction method of multipliers. Foundations and Trends in Machine Learning 3 (1), 1–122.

Cacchiani, V., Huisman, D., Kidd, M., Kroon, L., Toth, P., Veelenturf, L., Wagenaar, J., 2014. An overview of recovery models and algorithms for real-time railway rescheduling. Transportation Research Part B: Methodological 63 (2), 15–37.

Caimi, G., Fuchsberger, M., Laumanns, M., Lthi, M., 2007. A model predictive control approach for discrete-time rescheduling in complex central railway station areas. Computers and Operations Research 27 (3), 145–155.

Chang, C., Thia, B., 1996. Online rescheduling of mass rapid transit systems: fuzzy expert system approach. In: Electric Power Applications, IEE Proceedings-. Vol. 143. IET, pp. 307–316.

Corman, F., D' Ariano, A., Pacciarelli, D., Pranzo, M., 2012. Optimal inter-area coordination of train rescheduling decisions. Transportation Research Part E: Logistics and Transportation Review 48 (1), 71–88.

Corman, F., Meng, L., 2018. A review of online dynamic models and algorithms for railway traffic management. IEEE Transactions on Intelligent Transportation Systems 16 (3), 1274–1284.

Eberlein, X. J., Wilson, N. H. M., Bernstein, D., 2001. The holding problem with real–time information available. Transportation Science 35 (1), 1–18.

Fernandez, A., Cucala, A., Vitoriano, B., de Cuadra, F., 2006. Predictive traffic regulation for metro loop lines based on quadratic programming. Proceedings of the Institution of Mechanical Engineers, Part F: Journal of Rail and Rapid Transit 220 (2), 79–89.

Fonzone, A., Schmöcker, J., Liu, R., 2015. A model of bus bunching under reliability based passenger arrival patterns. Transportation Research Part C: Emerging Technologies 59, 164–182.

Goodman, C., Murata, S., 2001. Metro traffic regulation from the passenger perspective. Proceedings of the Institution of Mechanical Engineers, Part F: Journal of Rail and Rapid Transit 215 (2), 137–147.

Hollander, Y., Liu, R., 2008. Estimation of the distribution of travel times by repeated simulation. Transportation Research Part C: Emerging Technologies 16, 212–231.

Kang, L., Wu, J., Sun, H., Zhu, X., Wang, B., 2015. A practical model for last train rescheduling with train delay in urban railway transit networks. Omega 50, 29–42.

Kecman, P., Corman, F., D' Ariano, A., Goverde, R. M. P., 2013. Rescheduling models for railway traffic management in large-scale networks. Public Transport 5 (1-2), 95–123.

Li, S., Liu, R., Yang, L., Gao, Z., 2019. Robust bus controls considering delay disturbances and passenger demand uncertainty. Transportation Research Part B: Methodological 123, 88–109.

Li, S., Schutter, B. D., Yang, L., Gao, Z., 2016a. Robust model predictive control for train regulation in underground railway transportation. IEEE Transactions on Control Systems Technology 24 (3), 1075–1083.

Li, S., Yang, L., Gao, Z., Li, K., 2016b. Robust train regulation for metro lines with stochastic passenger arrival flow. Information Sciences 373, 287–307.

Li, S., Zhou, X., Yang, L., Gao, Z., 2018. Automatic train regulation of complex metro networks with transfer coordination constraints: A distributed optimal control framework. Transportation Research Part B: Methodological 117, 228–253.

Li, X., Lo, H. K., 2014. An energy-efficient scheduling and speed control approach for metro rail operations. Transportation Research Part B: Methodological 64, 73–89.

Lin, W., Sheu, J., 2010. Automatic train regulation for metro lines using dual heuristic dynamic programming. Proceedings of the Institution of Mechanical Engineers, Part F: Journal of Rail and Rapid Transit 224 (1), 15–23.

Lin, W., Sheu, J., 2011. Optimization of train regulation and energy usage of metro lines using an adaptive-optimal-control algorithm. IEEE Transactions on Automation Science and Engineering 8 (4), 855–864.

Mannino, C., Mascis, A., 2009. Optimal real-time traffic control in metro stations. Operations Research 57 (4), 1026–1039.

Moaveni, B., Najafi, S., 2018. Metro traffic modeling and regulation in loop lines using a robust model predictive controller to improve passenger satisfaction. IEEE Transactions on Control Systems Technology 26 (5), 1541–1551.

Schmöcker, J., Sun, W., Fonzone, A. and Liu, R., 2016. Bus bunching along a corridor served by two lines. Transportation Research Part B: Methodological 93, 300–317.

Sheu, J., Lin, W., 2012. Energy-saving automatic train regulation using dual heuristic programming. IEEE Transactions on Vehicular Technology 61 (4), 1503–1514.

Su, S., Tang, T., Roberts, C., 2015. A cooperative train control model for energy saving. IEEE Transactions on Intelligent Transportation Systems 16 (2), 622–631.

Timotheou, S., Panayiotou, C. G., Polycarpou, M. M., 2015. Distributed traffic signal control using the cell transmission model via the alternating direction method of multipliers. IEEE Transactions on Intelligent Transportation Systems 16 (2), 919–933.

Van Breusegem, V., Campion, G., Bastin, G., 1991. Traffic modeling and state feedback control for metro lines. IEEE Transactions on Automatic Control 36 (7), 770–784.

Vasirani, M., Ossowski, S., 2011. A computational market for distributed control of urban road traffic systems. IEEE Transactions on Intelligent Transportation Systems 12 (2), 313–321.

Wang, X., Li, S., Su, S., Tang, T., 2019. Robust fuzzy predictive control for automatic train regulation in high-frequency metro lines. IEEE Transactions on Fuzzy Systems 27 (6): 1295–1308.

Wu, W., Liu, R., Jin, W., 2016. Designing robust schedule coordination scheme for transit networks with safety control margins. Transportation Research B: Methodological 93, 495–519.

Wu, W., Liu, R. and Jin, W., 2017. Bus holding control strategies considering overtaking and passenger behaviour. Transportation Research Part B: Methodological 104, 175–197.

Wu, W., Liu, R., Jin, W., 2019. Stochastic bus schedule coordination considering demand assignment and rerouting of passengers. Transportation Research Part B: Methodological 121, 275–303.

Xun, J., Yin, J., Liu, R., Liu, F., Zhou, Y., Tang, T., 2019. Cooperative control of high-speed trains for headway regulation: A self-triggered model predictive control based approach. Transportation Research Part C: Emerging Technologies 102, 106–120.

Yao, Y., Zhu, X., Dong, H., Wang, S., Wu, H., Tong, L., Zhou, X., 2019. ADMM-based problem decomposition scheme for vehicle routing problem with time windows. Transportation Research Part B: Methodological 1297, 156–174.

Ye, H., Liu, R., 2016. A multiphase optimal control method for multi-train control and scheduling on railway lines. Transportation Research Part B: Methodological 93, 377–393

Ye, H., Liu, R., 2017. Nonlinear programming methods based on closed-form expressions for optimal train control. Transportation Research Part C: Emerging Technologies 82, 102–123.

Yin, J., Su, S., Xun, J., Tang T., Liu, R., 2020. Data-driven approaches for modelling train control models: Comparison and case studies. ISA Transactions 98, 349–363.

Yin, J., Yang, L., Tao, T., Gao, Z., Ran, B., 2017. Dynamic passenger demand oriented metro train scheduling with energy-efficiency and waiting time minimization: Mixed-integer linear programming approaches. Transportation Research Part B: Methodological 97, 182–213.

Zhang, H., Li, S., Yang, L., 2019. Real-time optimal train regulation design for metro lines with energy-saving. Computers and Industrial Engineering 127, 1282–1296.